Early-age cracking due to restraint: Laboratory and field investigations on the predictive capacity of the simplified method in Annex D of the future EC2

Antonia Menga, Jean-michel Torrenti, Terje Kanstad, Anja Birgitta Estensen Klausen

Received: 3 February 2024 | Revised: 10 April 2024 | Accepted: 28 April 2024

DOI: 10.1002/suco.202400173

ARTICLE

fib CEB-FIP WILEY

Early-age cracking due to restraint: Laboratory and field investigations on the predictive capacity of the simplified method in Annex D of the future EC2

Antonia Menga[1] | **Jean-Michel Torrenti**[2,3] | **Terje Kanstad**[1] | **Anja Birgitta Estensen Klausen**[1]

[1]Department of Structural Engineering, Norwegian University of Science and Technology (NTNU), Trondheim, Norway

[2]Materials and Structure Department, Université Gustave Eiffel, Paris, France

[3]ESITC-Paris, Arcueil, France

Correspondence
Antonia Menga, Department of Structural Engineering, NTNU, Materialteknisk, 3-235, Gløshaugen, Richard Birkelands vei 1a, 7034, Trondheim, Norway.
Email: antonia.menga@ntnu.no

Funding information
Electricité de France; Norges Teknisk-Naturvitenskapelige Universitet

Abstract

The Annex D of the future EC2 draft gives guidance on the evaluation of early-age cracking of large structures due to restraint. In case of restrained conditions, compressive stresses are firstly generated in massive structures due to temperature increase, then tensile stresses are generated due to temperature decrease and shrinkage. Due to these tensile stresses, there is a risk of cracking which may be evaluated by the simplified method in Annex D. This method is currently verified against laboratory tests performed in the temperature-stress testing machine and field cases on restrained concrete elements. The laboratory verification consisted of five approaches to consider different available input (modeled, assumed, or measured). The field investigation focused on the relation between the calculated cracking risk and the observed damage. The results show that the method has very good accuracy and captures with reasonable simplicity the mechanisms and the relations between the parameters involved.

KEYWORDS

concrete, cracking, early age, EC2, field test, restrained strains, SCMs, TSTM

1 | INTRODUCTION

Cracks influence the aesthetics, durability, and tightness of concrete structures, often resulting in economic and sustainability consequences.[1] It is therefore important to evaluate the cracking risk throughout the whole life span of a structure by accurate and relevant methods (e.g., References 2–5).

In this paper we consider the cracking risk (R_{cr}) of restrained concrete elements at early ages, as proposed by Annex D in Reference 2:

$$R_{cr}(t) = \frac{\sigma_{ct}(t)}{0.8 f_{ct,eff}(t)} \begin{cases} < 1 & \text{no cracking} \\ \geq 1 & \text{cracking} \end{cases} \quad (1)$$

where $\sigma_{ct}(t)$ is the maximum tensile stress in the element and $f_{ct,eff}(t)$ is the tensile strength at time t. The coefficient 0.8 is a safety factor accounting for sustained loading, in which case the coupling between creep and damage of concrete, in form of microcracking, rapidly reduces the concrete resistance. Several experimental evidences show that this coupling (tertiary creep) generally occurs when the stress is higher than 80% of the strength.[6]

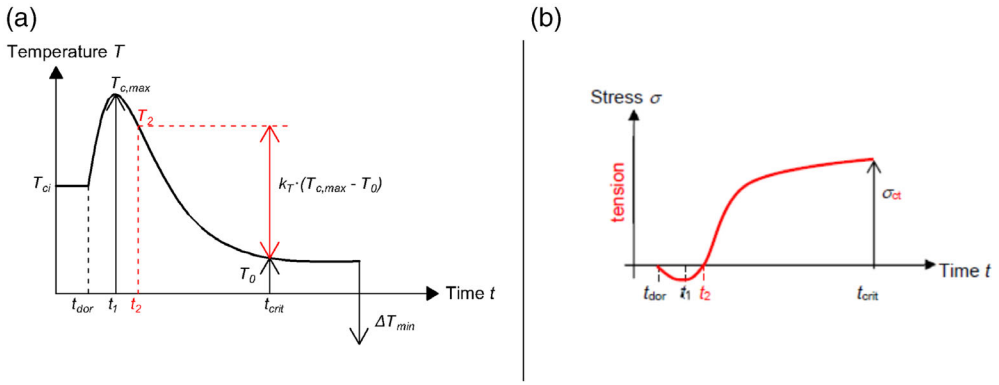

FIGURE 1 (a) Typical temperature history of a structural concrete element, and (b) related stress history.[1] Starting from the temperature of the fresh concrete (T_{ci}), the temperature increases due to the heat of hydration up to $T_{c,max}$ (heating phase). In the cooling phase, the temperature decreases until thermal equilibrium with the restraining structure (T_0) at time t_{crit}. Additional temperature drop (ΔT_{min}) due to daily and seasonal temperature variations is also considered. The restraining structure prevents the thermal expansion and following contraction of the newly cast concrete member, allowing for compressive and later tensile stresses to occur. The time when the generated stresses change from compression to tension is indicated with t_2. T_2 is the temperature of the concrete element at t_2, while t_{dor} is the start time for stress development.

The focus is on through-cracks, which involve the whole thickness of the element. They occur in case of restrained conditions and are strongly related to the temperature situation in a newly-cast concrete element: the temperature first increases due to the released heat of hydration and then drops until thermal equilibrium with the restraining system (Figure 1a). Simultaneously, the concrete expands in the heating phase and contracts in the cooling phase. Through-cracks typically occur in the latter, when the restrained thermal contraction produces tensile stresses (Figure 1b). For this reason, suggested measures to reduce through-cracking are based on the reduction of the restraint and/or the temperature difference between the concrete element and the restraining system.[1]

Through-cracks mostly affect massive structures with small surface-to-volume ratio, which makes negligible the drying of the structure and the dispersion of the hydration heat. As a result, drying shrinkage and drying creep are neglected and the concrete can be assumed to be in quasi-adiabatic conditions.

The phenomenon of early-age cracking (EAC) is however more complex than this. Self-induced volume changes are caused by thermal dilation (TD) but also by autogenous deformation (AD), a more general term to indicate basic shrinkage (autogenous contraction) and autogenous expansion. Basic shrinkage increases the tensile stress while autogenous expansion decreases it. Moreover, during the hardening phase, the concrete exhibits strong viscoelastic behavior and its mechanical properties develop rapidly, resulting in higher stiffness (hence higher stress) in the cooling than in the heating phase.

Therefore, the evaluation of $\sigma_{ct}(t)$ may be challenging. Time-dependent analyses can be used but are complex and not always convenient. Conversely, simplified methods (SMs) are generally easier to interpret, faster, and may be utilized as part of a more comprehensive solution regime.[7] However, their limits (e.g., assumptions, models simplification, applicability to new concretes[8,9]) must be clearly highlighted and considered.

The current paper is a combined and enhanced version of the conference papers,[10,11] presented at the 6th fib International Congress. The aim is to assess the SM for the evaluation of early-age and long-term cracking due to restraint, proposed in Annex D of Reference 2. In this paper, the method is considered in relation to early age only. It is briefly presented, and then verified and discussed against laboratory tests performed in the temperature-stress testing machine (TSTM), and field cases on restrained concrete elements. The paper concludes with an analysis of the cracking risk test results.

2 | THE SIMPLIFIED METHOD

Annex D of Reference 2 guides on the evaluation of early-age and long-term cracking due to restraint, proposing a SM to calculate R_{cr}. The method includes TD and AD as driving forces to EAC, considers creep through the age-adjusted effective E-modulus method,[12] and accounts for the boundary conditions with a degree of restraint ($R_{ax,1}$). This factor is defined as the stiffness of the restraining structural system (k) divided by the stiffness of the total system (Figure 2). $R_{ax,1}$ varies between 0 and 1, where 1 indicates a fully restrained system and 0 an unrestrained one.

$$R_{ax,1} = \frac{k}{E_c A_c + k}. \quad (2)$$

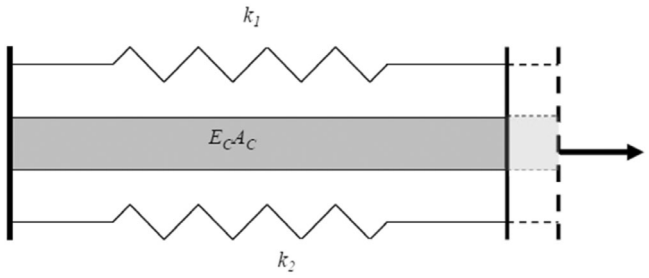

FIGURE 2 Illustration of the degree of restraint.[9] The structural system is represented by a concrete element with E-modulus E_c and cross-sectional area A_c, restrained by two springs (restraining system) of stiffness k_1 and k_2. The stiffness of the restraining system is hence $k = k_1 + k_2$.

Alternatively:

$$R_{ax,1} = 1 - \frac{\varepsilon_{restr}}{\varepsilon_{imp}}, \tag{3}$$

where ε_{restr} is the strain developed in the restrained element and ε_{imp} is the imposed strain. Input data to Equations (2) and (3) should be estimated with complex analyses, preferably including 3D realistic models.[9,13]

The degree of restraint in principle varies in time due to the E-modulus development, but experience has shown that the variation is small at early ages.[7,9] A constant value of $R_{ax,1}$ is thus assumed throughout the SM domain.

In SM, the compressive stress occurring in the heating phase is neglected, although its influence on the stress history is accounted for through the parameter t_2 where the stress changes from compression to tension. Furthermore, the tensile stress in the cooling phase is assumed constant and totally applied in one step at t_2 (Figure 1). As for the strain, contraction is assumed positive and expansion negative since the concrete contracts in the cooling phase.

In this paper, the method is applied to the early-age case only, at the time when temperature-equilibrium between the restrained and restraining structural concrete member is achieved (t_{crit}). The corresponding stress generated inside the newly-cast element, $\sigma_{ct}(t_{crit})$, is expressed by the following equation:

$$\sigma_1(t_{crit}) = R_{ax,1}\frac{E_c(t_2)}{1+\chi\varphi_{st}}\Big\{k_{Temp}\alpha_{cth}(T_{c,max} - T_0) + [\varepsilon_{cbs}(t_{crit}) - \varepsilon_{cbs}(t_2)]\Big\}, \tag{4}$$

where $\chi\varphi_{st}$ accounts for short-term creep relaxation, significant due to the low maturity of concrete and the presence of hydration heat. Annex D suggests a value of 0.55.$E_c(t_2)$ is the modulus of elasticity of concrete at time t_2. t_2 is the time when the tensile stress is applied according to SM, corresponding to the time of stress change from compression to tension. Annex D suggests a value of 2 days if no experimental value is provided. α_{cth} is the coefficient of thermal expansion of concrete. Annex D suggests a value of $10 \times 10^{-6}\,^{\circ}C^{-1}$ if no experimental value is provided. $k_{Temp}(T_{c,max} - T_0) = (T_2 - T_0) = \Delta T$ is the part of the temperature decrease causing tensile stresses. k_{Temp} is a thermal factor accounting for the reduction in temperature from $T_{c,max}$ to T_2 (see Figure 1), and may be taken as 0.9. $k_{Temp}\alpha_{cth}(T_{c,max} - T_0)$ is the TD in the cooling phase. $[\varepsilon_{cbs}(t_{crit}) - \varepsilon_{cbs}(t_2)] = \Delta AD$ is the AD of the concrete between t_2 and t_{crit}. TD + AD is the total volume changes or total free deformation (FD).

3 | LABORATORY VERIFICATION

In this section, SM is applied to results of laboratory tests from the literature, suited for the determination of self-induced stress at early ages. The tests are grouped in a reference database, against which the method is verified according to five approaches that consider the availability of input in practical applications.

The results of the laboratory verification are discussed at the end of the section.

3.1 | Reference database

The numerous factors involved, make the phenomenon of through-cracking quite challenging to be reproduced in the laboratory. Nevertheless, various test methods are described in the literature[14–16] (plate test, substrate restrained test, ring test, longitudinal test). Among them, the TSTM test is recognized as the most advanced and reliable one.[17] It is in fact able to measure the strain and stress development of a concrete element under varying temperature, restraint, and curing conditions (sealed or drying), allowing for the evaluation of the crack sensitivity of cementitious mixes. The TSTM can also be used to test fiber reinforced and reinforced concrete (see for instance References 18,19) although studies in this field (especially reinforced concrete) are scarce.[15] Other applications of the TSTM test include monitoring of elastic and viscoelastic properties from setting time, and testing of concrete in its plastic state.[16]

A TSTM (Figure 3) is a longitudinal restraining device consisting of a metal formwork with a fixed and a movable end. The movable end can return to its original position periodically, once a certain deformation threshold is reached. This is achieved by a screw or a hydraulic mechanism manually or automatically activated. The force

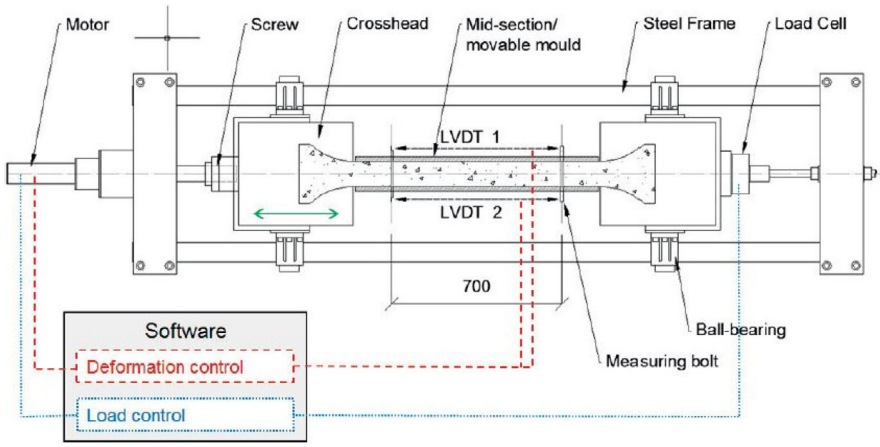

FIGURE 3 Scheme of the TSTM at the Norwegian University of Science and Technology.[20]

induced during such an operation is measured by a load cell or is computed from a deformation measurement of the rig. A TSTM system usually comprises a restrained rig with enlarged ends and an unrestrained rig used for the measurement of FD in which the concrete can be directly cast. Both rigs are generally provided with a temperature-control system.

TSTM systems are sophisticated and expensive, and not many institutes have the resources to afford one. The equipment is also difficult to control, operate, and maintain, and cannot be found on the market, so it must be manufactured. As a result, there are not many TSTMs worldwide (about 22[15]), and even though they have similar operating principle and test set-up, they also have differences about the custom-made parts and mechanisms (e.g., sensors type and positioning, size of specimen).

In this study, selected TSTM tests found in the literature are used to build a reference database to verify SM.

The database covers 58 tests which meet the following criteria:

- The test is conducted on unreinforced concrete.
- The test occurred in sealed conditions, under varying temperature (adiabatic and semi-adiabatic temperature histories are preferred). The value of $T_{c,max} - T_0$ must be stated or be deductible. Cases with temperature below 0°C are excluded.
  Isothermal tests are excluded because, even though SM could be applied assuming $t_2 = t_{dor}$, it would result $E_c(t_2) = E_c(t_{dor}) = 0$, making the method de facto not applicable.
- $R_{ax,1}$ is kept constant throughout the test.
- The mechanical properties of the concrete (compressive strength, tensile strength, and E-modulus) at different ages are provided.
- FD is measured and/or the deduced AD is provided.
- Stated or deductible values of t_2, t_{crit}, and $\sigma_1(t_{crit})$ are provided.

The tests are grouped in investigations, in turn arranged according to the institute they belong to (Table 1): Norwegian University of Science and Technology (NTNU), Tsinghua University (TU), Hohai University (HU), Institute of Water Resources and Hydropower Research (IWHR), and University of Tokyo (UTokyo). Each of the institutes is equipped with a unique TSTM system, described in Table 2.

The values of the input parameters for SM are reported in Table 3 for each test. They are:

- mean compressive strength at 28 days, $f_{cm}(28d)$;
- degree of restraint, $R_{ax,1}$;
- coefficient of thermal expansion, α_{cth};
- starting time of the generated tensile stress, t_2;
- time at failure or time at thermal equilibrium between the restrained structure and the restraining system[7] (t_{crit});
- E-modulus at time t_2, $E_c(t_2)$;
- Temperature variation causing the tensile stress, $T_{c,max} - T_0$;
- AD variation from t_2 to t_{crit}, $\varepsilon_{cbs}(t_{crit}) - \varepsilon_{cbs}(t_2)$.

Table 3 also includes experimental values of $\sigma_{ct}(t_{crit})$ and $f_{ct,eff}(t_{crit})$. The effective tensile strength is taken as the mean tensile strength of direct tension tests according to Reference 2. In cases where the tensile strength was measured through splitting tests, the splitting strength values (f_{ts}) have been converted to direct strength values (f_t) according to Reference 46:

$$f_t = 0.79 \cdot f_{ts} + 0.53 \quad \text{test on } 100 \times 200 \text{ mm cylinders}, \tag{5}$$

TABLE 1 Summary of the investigations included in the reference database.

Institute	Investigation	Concrete type	Number of tests
Norwegian University of Science and Technology, NTNU (Norway)	Bjøntegaard[21]	OPC, FA, SF	9
	Klausen[20]	OPC, FA	4
	Cementa[22–26]	OPC, FA	5
	Schwenk[27,28]	GGBFS	2
	VPI[29–31]	OPC, VPI	3
Tsinghua University, TU (China)	Tao and Weizu[32]	OPC, SF, FA	3
	Zhu et al.[33]	OPC, FA	5
Hohai University, HU (China)	Shen et al.[34]	OPC, GGBFS	4
	Shen et al.[35]	OPC, SF	4
Institute of Water Resources and Hydropower Research, IWHR (China)	Xin et al.[36]	FA	6
	Xin et al.[37]	OPC, FA	4
University of Tokyo, UTokyo (Japan)	Lim et al.[38]	OPC, FA, GGBFS, EA	4
	Ou et al.[39]	OPC	2
	Ou et al.[40]	OPC	1
	Ou et al.[41]	OPC, EA	2
Total	15	OPC, FA, SF, GGBFS, VPI, EA	58

Note: Each investigation is associated to the number of tests considered in the present work and to the related concrete type containing: Portland cement (OPC), fly ash (FA), silica fume (SF), ground granulated blast furnace slag (GGBFS), volcanic pozzolan from Iceland (VPI), or expansive agent (EA).

$$f_t = 0.77 \cdot f_{ts} + 0.21 \quad \text{test on 100 mm cubes.} \tag{6}$$

Table 3 shows only the direct strength values. Additionally, it indicates if the tests failed, and whether the data were explicitly stated in the literature, assumed according to Annex D, or deduced by the authors.

Tables 2 and 3 show that the tests included in the database were performed using different (but analogous) TSTM systems, approaches, and materials, considerably influencing the test results. Nevertheless, a representative and homogeneous database is necessary to evaluate SM. Therefore, the database was checked for the presence of outliers before proceeding to the verification of SM through the Hampel's test (described in Reference 47). This test is quite simple, has very good efficiency in finding even mild outliers,[47] and has been successfully applied to a Round-Robin investigation on early-age concrete.[48] No outliers were found in the current database.

3.2 | Verification approaches

Available input may vary in the practical application of SM. To consider this, five verification approaches were introduced in Table 4. The approaches are explained in the following, and their results are presented and discussed in Section 3.3.

In the *first approach*, the input parameters are experimentally determined, except for α_{cth} assumed to be $10 \times 10^{-6}\,°C^{-1}$ according to Annex D, and AD, modeled according to the basic shrinkage formula in Reference 2:

$$\varepsilon_{cbs}(t) = \varepsilon_{cbs,f_{cm}} \cdot \beta_{bs,t} \cdot \alpha_{NDP,b}, \tag{7}$$

where $\alpha_{NDP,b}$ is a Nationally Determined Parameter assumed equal to 1 in the current study;

$$\beta_{bs,t} = 1 - \exp\left(-0.2\sqrt{t}\right) \tag{8}$$

is a time-development function;

$$\varepsilon_{cbs,f_{cm}} = -\alpha_{bs}\left(\frac{f_{cm,28}}{60 + f_{cm,28}}\right)^{2.5} \cdot 10^{-6} \tag{9}$$

is the basic shrinkage coefficient; α_{bs} is a coefficient which depends on the early strength development of concrete (Table B.3 in Reference 2), which is related to the concrete class (Table D.1 in Reference 2). This in turn depends on the concrete characteristic compressive strength f_{ck} and given values of t_{dor}.

The *second approach* is taken from References 1,10. It is identical to the first one with the exception that t_2 is assumed to be 2 days (value according to Reference 2 and

TABLE 2 Comparison between the TSTM systems considered in the study.

Institute	Dimensions	Measuring system	Operation
NTNU (Norway)[8,20,21,42]	Dog-bone shape. *Measuring length*: 700 mm *Total length*: 1000 mm *Central cross-section*: 88 × 100 mm^2 *FD specimen*: prism,100 × 100 × 460 mm^3	*Deformation*: LVDTs in contact with steel rods embedded at the end of the measuring length. *Deformation threshold*: 6 μm *Load*: load cell with accuracy 0.2 kN on the fixed crosshead. *Temperature*: measured by a thermocouple in the center of the specimen. Thermal regulation by water circulation in the mold.	*Before casting*: two plastic layers with talcum in-between placed in the molds. *After casting*: sampled covered with plastic layers and aluminum foil to obtain sealed conditions. *Start time*: after setting.
TU (China)[32,33,43]	Dog-bone shape. *Measuring length*: 1000 mm *Total length*: 2000 mm *Central cross-section*: 100 × 100 mm^2 *FD specimen*: identical multi-TSTM system (4 rigs).	*Deformation*: LVDTs in contact with steel rods vertically embedded in the measuring length. *Deformation threshold*: 2 μm *Temperature*: temperature-controlled environment.	*After casting*: sealed conditions. *Start time*: 25 h, but the displacement of the movable crosshead is measured from casting.
HU (China)[34,35,44]	Dog-bone shape. *Measuring length*: 1500 mm *Central cross-section*: 10 × 150 mm^2 *FD specimen*: identical.	*Deformation*: LVDT on the restrained crosshead specimen and steel frame. *Deformation threshold*: 3 μm *Temperature*: controlled by a sensor embedded in the specimen. Thermal regulation by water circulation in the mold.	*Before casting*: thin vinyl sheet placed in the molds. *After casting*: sample covered with plastic sheet to obtain sealed conditions. *Start time*: immediately after casting.
IWHR (China)[36,37]	Dog-bone shape. *Measuring length*: 1000 mm *Total length*: 1500 mm *Central cross-section*: 150 × 150 mm^2 *FD specimen*: identical.	*Deformation*: LVDTs in contact with steel rods embedded at the end of the measuring length. *Load*: load cell with accuracy 0.1 kN. *Temperature*: thermal regulation by glycol circulation in the mold.	*Start time*: after setting.
UTokyo (Japan)[38–41]	Dovetail shaped crossheads. *Measuring length*: 1200 mm *Central cross-section*: 120 × 120 mm^2 *FD specimen*: identical.	*Deformation*: LVDTs in contact with steel rods between the crossheads. *Deformation threshold*: 0.5 μm *Load*: Two load cells at the crossheads. *Temperature*: Four platinum resistance thermometers inside the specimen. Thermal regulation by a temperature chamber with circulating air.	*Before casting*: two plastic layers placed in the molds. *After casting*: sample covered with a slightly wet cloth and wrapped with two layers of plastic. 24 h later, the lateral and bottom molds were separated from the beam to reduce friction. *Start time*: 24 hours.

Note: More details can be found in the referred literature.

deriving from the average of measured t_2 values from various experimental results, e.g., References 20,21). The approach showed good accuracy when verified against Cementa (2019) test results,[10] so the aim of the current paper is to verify whether 2 days appropriately estimates t_2 in a broader and more various database, especially for concretes with high AD development before 1 day (as in References 21,34,35). In fact, SM neglects FD in the heating phase (before t_2) and only uses FD produced in the cooling phase (after t_2) as driving force to $\sigma_1(t_{crit})$. Assuming a low value of t_2 will thus increase this driving force but will conversely decrease $E_c(t_2)$.

TD is calculated as $k_{Temp}(T_{c,max} - T_0)$ in all cases, resulting independent of t_2 variations, which are

TABLE 3 Experimental values of the input parameters for SM, of the maximum tensile stress, and of the effective tensile strength (taken as mean tensile strength of direct tension test results according to Reference 2) of the tests included in the reference database.

Institute	Investigation	Test ID	w/b (−)	$f_{cm}(28d)$ (MPa)	$R_{ax,1}$ (−)	α_{cth} ($\times 10^{-6}$ °C^{-1})	t_2 (days)	t_{crit} (days)	$E_c(t_2)$ (MPa)	$T_{c,max} - T_0$ (°C)	$\varepsilon_{cbs}(t_{crit}) - \varepsilon_{cbs}(t_2)$ ($\times 10^{-6}$)	$\sigma_1(t_{crit})$ (MPa)	$f_{ct,eff}(t_{crit})$ (MPa)	Failure
NTNU (Norway)	Bjøntegaard (1999)	NTNU01_01_OPC	0.40	60.56	1.00	9.50	1.76	3.43	26,000	21.00	−15.00	3.00	3.70	Yes
		NTNU01_02_OPC	0.40	53.92	1.00	10.00	1.29	2.86	20,000	20.00	36.00	2.80	3.83[a]	Yes
		NTNU01_03_20%SF	0.23	112.00	1.00	11.50	1.00	1.54	38,500[a]	3.70	151.00	4.70	5.46[a]	Yes
		NTNU01_04_20%FA	0.40	53.60	1.00	10.50	1.38	2.48	25,000	13.50	41.00	2.90	4.21[a]	Yes
		NTNU01_05_5%SF	0.40	63.68	1.00	10.00[a]	1.53	2.35	27,000	16.00	25.00	3.00	3.30	Yes
		NTNU01_06_10%SF	0.40	70.40	1.00	10.00[a]	1.23	1.88	29,000	12.00	61.00	3.00	3.09[a]	Yes
		NTNU01_07_5%SF	0.40	63.68	1.00	10.00[a]	1.06	8.00	25,000	19.00	19.00	3.00	3.30	Yes
		NTNU01_08_10%SF	0.40	70.40	1.00	10.00[a]	1.06	5.23	27,000	16.00	54.00	3.10	3.09[a]	Yes
		NTNU01_09_5%SF	0.40	63.68	1.00	10.00[a]	1.20	2.50	26,000	12.00	54.00	3.17	3.30	Yes
	Klausen (2016)	NTNU02_01_OPC	0.40	64.24	0.50	9.00	2.96	6.75	31,800	42.00	−16.00	3.26	3.53	No
		NTNU02_02_17%FA	0.40	56.96	0.50	9.10	3.17	6.00	30,100	32.00	27.00	3.08	2.99	Yes
		NTNU02_03_25%FA	0.40	52.56	0.50	9.00	3.29	7.00	29,700	29.00	25.00	3.00	2.89	No
		NTNU02_04_33%FA	0.40	42.88	0.50	9.20	3.58	9.00	29,000	25.00	15.00	2.32	2.75	No
	Cementa (2019)	NTNU03_01_OPC	0.38	56.64	0.50	9.80	3.00	9.25	34,200	41.80	−1.61	4.00	4.80	No
		NTNU03_02_20%FA	0.38	52.88	0.50	9.60	3.00	9.25	32,600	36.20	7.10	3.75	4.50	No
		NTNU03_03_OPC	0.38	48.96	0.50	9.60	3.00	9.25	32,800	39.50	6.00	3.50	4.00	No
		NTNU03_04_OPC	0.48	45.52	0.50	9.20	3.20	9.25	30,800	35.20	−14.00	2.80	4.30	No
		NTNU03_05_20%FA	0.48	37.12	0.50	9.60	3.00	9.25	28,900	28.80	−11.30	2.55	3.30	No
	Schwenk (2022)	NTNU04_01_30% GGBFS	0.45	65.84	0.50	11.00	2.50	4.08	24,500	38.00	20.90	2.88	3.31	Yes
		NTNU04_02_70% GGBFS	0.45	57.12	0.50	10.20	1.75	4.50	20,200	23.00	143.00	3.50	3.92	Yes
	VPI (2023)	NTNU05_01_OPC	0.40	74.40	0.30	9.50	2.25	5.75	39,200	40.00	48.30	3.50	4.41	Yes
		NTNU05_02_17% VPI	0.40	70.40	0.30	10.00	2.21	4.54	36,000	33.00	59.10	3.20	3.81	Yes
		NTNU05_03_33% VPI	0.40	56.80	0.30	9.80	2.46	5.46	38,700	30.00	73.70	3.60	3.40	Yes
TU (China)	Tao and Weizu (2006)	TU01_01_OPC	0.35	72.00	1.00	10.00[b]	1.13	4.00	19,900	19.00	13.00[a]	2.25	4.80[a]	No
		TU01_01_6%SF	0.35	76.00	1.00	10.00[b]	0.75	4.00	20,200	20.00	43.00[a]	3.15	5.00[a]	No
		TU01_01_30%FA	0.35	56.00	1.00	10.00[b]	1.13	4.00	18,400	16.00	−16.00[a]	1.60	3.96[a]	No

(Continues)

TABLE 3 (Continued)

Institute	Investigation	Test ID	w/b (−)	$f_{cm}(28d)$ (MPa)	$R_{ax,1}$ (−)	α_{cth} ($\times 10^{-6}$ °C^{-1})	t_2 (days)	t_{crit} (days)	$E_c(t_2)$ (MPa)	$T_{c,max} - T_0$ (°C)	$\varepsilon_{cbs}(t_{crit}) - \varepsilon_{cbs}(t_2)$ ($\times 10^{-6}$)	$\sigma_1(t_{crit})$ (MPa)	$f_{ct,eff}(t_{crit})$ (MPa)	Failure
	Zhu et al. (2020)	TU02_01_35%FA	0.50	29.26[a]	1.00[b]	10.00[b]	3.75	7.71	30,400[a]	4.88	19.60[a]	1.41	1.65	Yes
		TU02_02_35%FA	0.50	30.76[a]	1.00[b]	10.00[b]	6.67	8.33	30,800[a]	8.91	−12.00[a]	1.45	1.74	Yes
		TU02_03_OPC	0.50	31.09[a]	1.00[b]	10.00[b]	7.92	8.75	30,900[a]	8.14	−19.00[a]	1.54	1.76	Yes
		TU02_04_35%FA	0.50	25.01[a]	1.00[b]	10.00[b]	5.83	8.13	29,000[a]	5.61	−3.00[a]	1.19	1.38	Yes
		TU02_05_35%FA	0.50	22.82[a]	1.00[b]	10.00[b]	7.08	7.71	28,200[a]	6.38	0.00[a]	1.10	1.23	Yes
HU (China)	Shen et al. (2020a)	HU01_01_OPC	0.32	60.47	1.00	4.38	2.36	4.46	33,700	41.56	−3.00	3.21	4.06	Yes
		HU01_02_20% GGBFS	0.32	56.17	1.00	5.58	1.80	4.21	31,700	31.56	−16.00	3.02	3.73	Yes
		HU01_03_35% GGBFS	0.32	52.08	1.00	6.70	1.58	3.83	30,000	21.37	27.00	2.88	3.55	Yes
		HU01_04_50% GGBFS	0.32	49.21	1.00	6.56	1.50	3.63	28,400	19.01	33.00	2.79	3.30	Yes
	Shen et al. (2020b)	HU02_01_OPC	0.33	48.72	0.50[a]	6.44	2.86	4.46	35,300	40.60	−6.00	2.20	3.71	Yes
		HU02_02_5%SF	0.33	53.20	0.50[a]	6.30	2.79	4.25	36,400	34.90	−2.00	2.12	3.92	Yes
		HU02_03_10%SF	0.33	57.52	0.50[a]	6.13	2.83	4.13	39,000	33.90	−10.00	2.10	4.18	Yes
		HU03_04_15%SF	0.33	59.12	0.50[a]	7.10	2.75	4.00	39,500	26.90	0.00	2.02	4.25	Yes
IWHR (China)	Xin et al. (2018)	IWHR01_01_35%FA	0.50	55.56[a]	1.00	7.50	5.79	10.67	36,800	9.32	−7.91[a]	1.14	1.53	Yes
		IWHR01_02_35%FA	0.50	55.56[a]	0.75	7.50	5.79	10.88	36,800	11.10	−6.93[a]	1.18	1.55	Yes
		IWHR01_03_35%FA	0.50	55.56[a]	0.50	7.50	5.79	11.33	36,800	15.70	−2.98[a]	1.12	1.57	Yes
		IWHR01_04_35%FA	0.50	55.56[a]	1.00	7.50	7.13	10.63	36,800	6.50	−7.88[a]	1.10	1.52	Yes
		IWHR01_05_35%FA	0.50	55.56[a]	0.75	7.50	6.71	10.83	36,800	9.23	−6.30[a]	1.14	1.53	Yes
		IWHR01_06_35%FA	0.50	55.56[a]	0.50	7.50	6.71	11.13	36,800	13.88	0.31[a]	0.95	1.54	Yes
	Xin et al. (2022)	IWHR02_01_OPC	0.45	35.04	1.00	7.90	3.42	6.13	37,500	14.40	−12.40[a]	1.78	2.52	Yes
		IWHR01_02_20%FA	0.45	26.64	1.00	8.00	3.42	6.54	35,000	12.90	−16.90[a]	1.63	2.37	Yes
		IWHR01_03_50%FA	0.45	17.52	1.00	7.60	3.42	8.88	20,000	12.70	−7.87[a]	0.95	0.83	Yes
		IWHR01_04_80%FA	0.45	8.72	1.00	7.10	3.88	8.21	10,500	6.60	−9.17[a]	0.33	0.67	Yes
UTokyo (Japan)	Lim et al. (2009)	UTokyo01_01_OPC	0.45	34.40	1.00	10.00[b]	2.08	7.92	15,000	35.00	−35.00[a]	2.75	2.66	Yes
		UTokyo01_02_30% FA	0.45	32.06	1.00	10.00[b]	2.08	7.08	17,500	26.00	1.00[a]	2.40	2.50	Yes

TABLE 3 (Continued)

Institute	Investigation	Test ID	w/b (−)	$f_{cm}(28d)$ (MPa)	$R_{ax,1}$ (−)	α_{cth} ($\times 10^{-6}$ °C^{-1})	t_2 (days)	t_{crit} (days)	$E_c(t_2)$ (MPa)	$T_{c,max} - T_0$ (°C)	$\varepsilon_{cbs}(t_{crit}) - \varepsilon_{cbs}(t_2)$ ($\times 10^{-6}$)	$\sigma_1(t_{crit})$ (MPa)	$f_{ct,eff}(t_{crit})$ (MPa)	Failure
		UTokyo01_03_45% GGBFS	0.45	32.06	1.00	10.00[b]	2.08	5.63	14,000	27.50	2.50[a]	2.80	2.50	Yes
		UTokyo01_04_7.5% EA	0.45	36.51	1.00	10.00[b]	1.67	6.88	18,000	35.00	−75.00[a]	2.35	2.80	Yes
	Ou et al. (2021)	UTokyo02_01_OPC	0.45	53.00[a]	1.00	10.00[b]	1.67	2.50	17,400	10.50	−9.50[a]	1.25	2.66[a]	Microcracking
		UTokyo02_02_OPC	0.45	53.00[a]	1.00	10.00[b]	2.13	2.13	23,000	6.50	41.50[a]	1.30	2.66[a]	Microcracking
	Ou et al. (2023a)	UTokyo03_01_OPC	0.45	48.30	1.00	10.00[b]	1.67	2.08	17,500	5.00	25.00[a]	0.90	2.47[a]	Microcracking
	Ou et al. (2023b)	UTokyo04_01_OPC	0.45	37.70	1.00	10.00[b]	1.25	5.00	16,500	25.00	25.00[a]	2.50	2.88[a]	No
		UTokyo04_02_10% EA	0.45	40.54	1.00	10.00[b]	1.75	5.00	19,000	25.00	−105.00[a]	1.50	3.06[a]	No

Note: Each test is identified by the code "XXyy_zz_mix," where "XX" represents the institute, "yy" is the number of the investigation in the institute, "zz" is the number of the test in the investigation, and "mix" is the type of concrete mix studied in the test. Contraction is indicated by positive values of $\varepsilon_{cbs}(t_{crit}) - \varepsilon_{cbs}(t_2)$.

[a]Values assumed according to Annex D.[2]

[b]Values deducted by the authors from data given in the reviewed literature. The 28 days value of f_{cm}, E_c, and/or $f_{ct,eff}$ is calculated according to Table 3.1 in Reference 45 from one of these values provided in the reference paper. From this, $E_c(t_2)$ and $f_{ct,eff}(t_{crit})$ are estimated. Moreover, for cases where the tensile strength was measured by splitting tests, the splitting values have been converted to direct tension values according to Equations (5) and (6)[46] prior to the calculation according to Table 3.1 in Reference 45.

$\varepsilon_{cbs}(t_{crit}) - \varepsilon_{cbs}(t_2)$ is calculated by subtracting TD from the measured free strain.

TABLE 4 Verification approaches.

Approaches	1st	2nd	3rd	4th	5th
Experimental values	t_2 t_{crit} $T_{c,max} - T_0$ $E_c(t_2)$	t_{crit} $T_{c,max} - T_0$ $E_c(t_2)$	t_2 t_{crit} $T_{c,max} - T_0$ $E_c(t_2)$ $\boldsymbol{\varepsilon_{cbs}(t_{crit}) - \varepsilon_{cbs}(t_2)}$	t_2 t_{crit} $T_{c,max} - T_0$ $E_c(t_2)$ $\boldsymbol{\alpha_{cth}}$	t_2 t_{crit} $T_{c,max} - T_0$ $E_c(t_2)$ $\boldsymbol{\alpha_{cth}}$ $\boldsymbol{\varepsilon_{cbs}(t_{crit}) - \varepsilon_{cbs}(t_2)}$
Assumed values	$\alpha_{cth} = 10^{-5}\,°C^{-1}$	$\alpha_{cth} = 10^{-5}\,°C{-}1$ $\boldsymbol{t_2 = 2\ days}$	$\alpha_{cth} = 10^{-5}\,°C^{-1}$	–	–
Modeled values	$\varepsilon_{cbs}(t_{crit}) - \varepsilon_{cbs}(t_2)$	$\varepsilon_{cbs}(t_{crit}) - \varepsilon_{cbs}(t_2)$	–	$\varepsilon_{cbs}(t_{crit}) - \varepsilon_{cbs}(t_2)$	–

Note: The assumptions characterizing each approach are reported in bold.

considered in $k_{Temp} = 0.9$ for simplicity reasons. Taking this into account and manipulating Equation (4), the following relation between $E_c(t_2)$, AD, and $\sigma_1(t_{crit})$ is obtained:

$$\sigma_1(t_{crit}) = C_1[E_c(t_2)] + C_2[E_c(t_2) \cdot \Delta AD], \tag{10}$$

where

$$C_1 = R_{ax,1}\frac{TD}{1+\chi\varphi_{st}}, \tag{11}$$

$$C_2 = R_{ax,1}\frac{1}{1+\chi\varphi_{st}}, \tag{12}$$

$C_1 > C_2$ are positive coefficients (in the cooling phase) which stay constant between the first and the second approaches. This means that $\sigma_1(t_{crit})$ changes according to how E_c and ΔAD vary between the approaches, and that E_c has a greater weight in the stress production.

Assuming a monotonous increasing development of AD in the cooling phase, the following is expected:

- For $t_{2exp} < 2$ days, the second approach gives higher values of E_c and lower values of ΔAD than the first approach. We thus expect *higher stress in the second approach*, almost proportional to the E_c increase, which in turn depends on t_{2exp} and on the exponential development of E_c.
- For $t_{2exp} > 2$ days, the second approach returns lower values of E_c and higher values of ΔAD than the first approach. We thus expect *lower stress in the second approach*.

The *third approach* evaluates the influence of the modeled AD on the stress development in hardening concrete. To do so, the first approach is modified to consider experimental values of AD.

The *fourth approach* evaluates the influence of the assumed α_{cth} on the stress development in hardening concrete. To do so, the first approach is modified to consider experimental values of α_{cth}.

In the *fifth approach* all input parameters are experimentally determined.

The mentioned approaches were chosen to investigate the key parameters involved in the production of $\sigma_1(t_{crit})$. In fact, assuming the first approach as reference, the second approach studies t_2 (or better $E_c(t_2)$), the third AD, the fourth α_{cth} (hence TD), and the fifth FD.

3.3 | Results and discussion

In this section, SM is applied to the reference database according to the five approaches. The results are shown in Figures 4–8 and Table 5.

The figures show the ratio (θ) between the stress calculated according to the approach considered and the corresponding experimental value for each test data. For $\theta > 1$ ($\theta < 1$), the approach overestimates (underestimates) $\sigma_1(t_{crit})$ and R_{cr}.

Table 5 reports the average value (μ_θ) and the standard deviation (s_θ) of θ, calculated according to the five approaches for each investigation and institute.

3.3.1 | The first approach

Considering the whole database, the first approach predicts $\sigma_1(t_{crit})$ very well in average, but with high s_θ (0.43), evident in Figure 4 especially for results coming from HU and UTokyo.

The stress of the tests conducted at NTNU is slightly underestimated by this approach ($\mu_\theta = 0.87$), yet the distribution is satisfactory ($s_\theta = 0.24$). In Figure 4, tests NTNU01_03_20%SF ($\theta = 0.22$) and NTNU04_02_70%

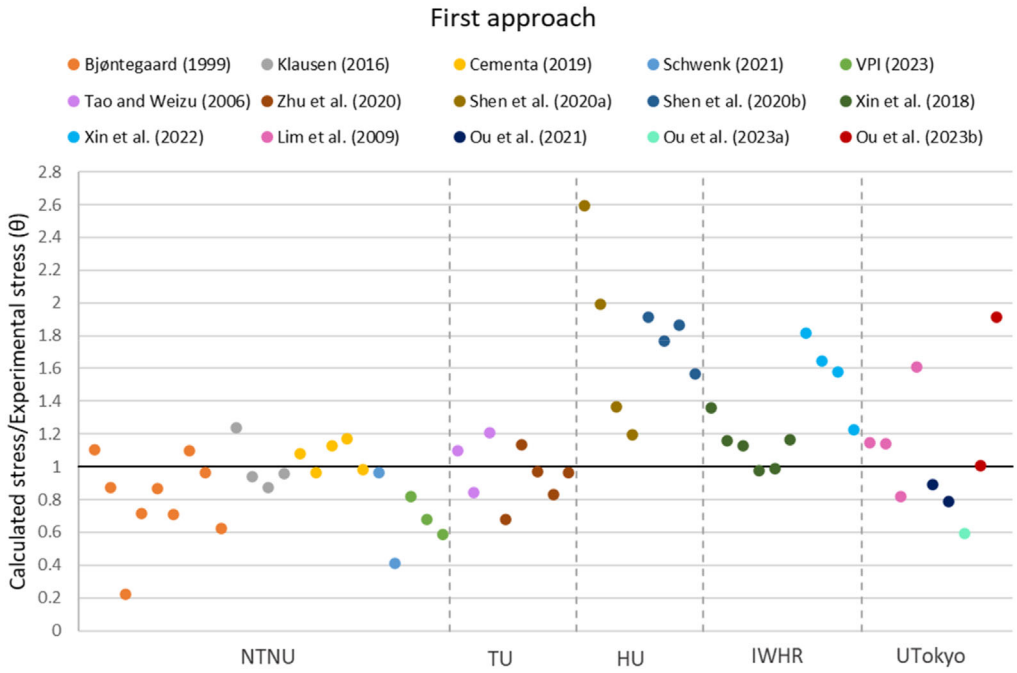

FIGURE 4 Calculated-to-experimental-stress ratio (θ) of the tests included in the reference database according to the first approach. The approach overestimates (underestimates) the experimental stress for $\theta > 1$ ($\theta < 1$). The tests are grouped in investigations (listed in the upper part of the figure), which are in turn arranged according to the institute they belong to. The reference institutes are separated by vertical dotted lines.

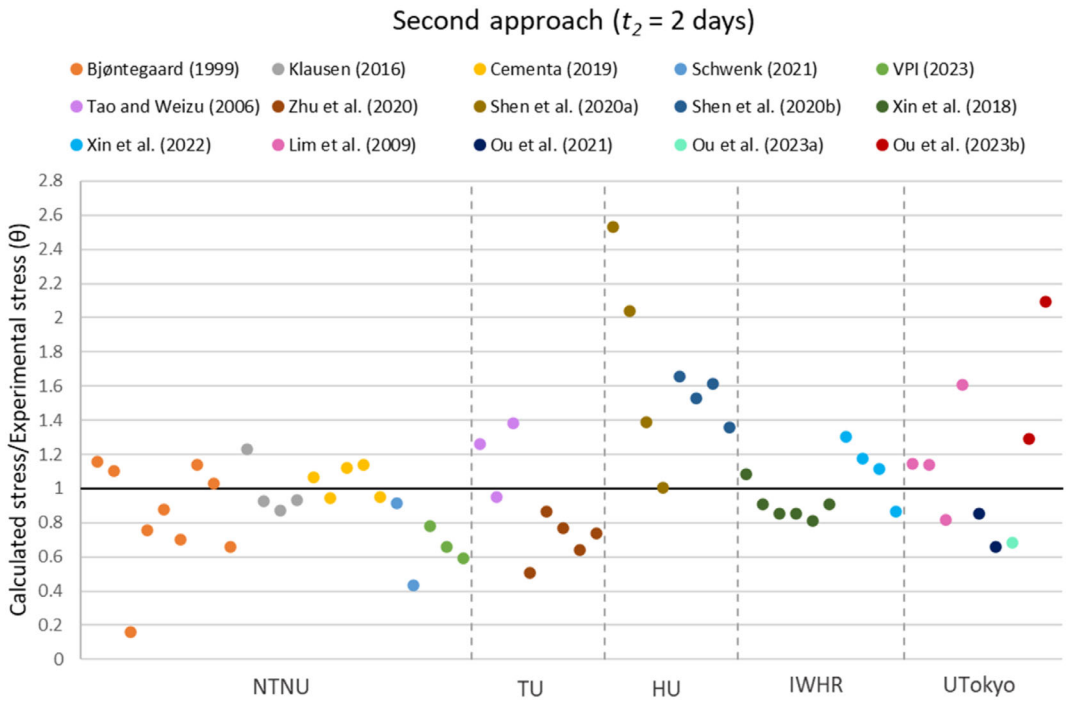

FIGURE 5 Calculated-to-experimental-stress ratio (θ) of the tests included in the reference database according to the second approach. The approach overestimates (underestimates) the experimental stress for $\theta > 1$ ($\theta < 1$). The tests are grouped in investigations (listed in the upper part of the figure), which are in turn arranged according to the institute they belong to. The reference institutes are separated by vertical dotted lines.

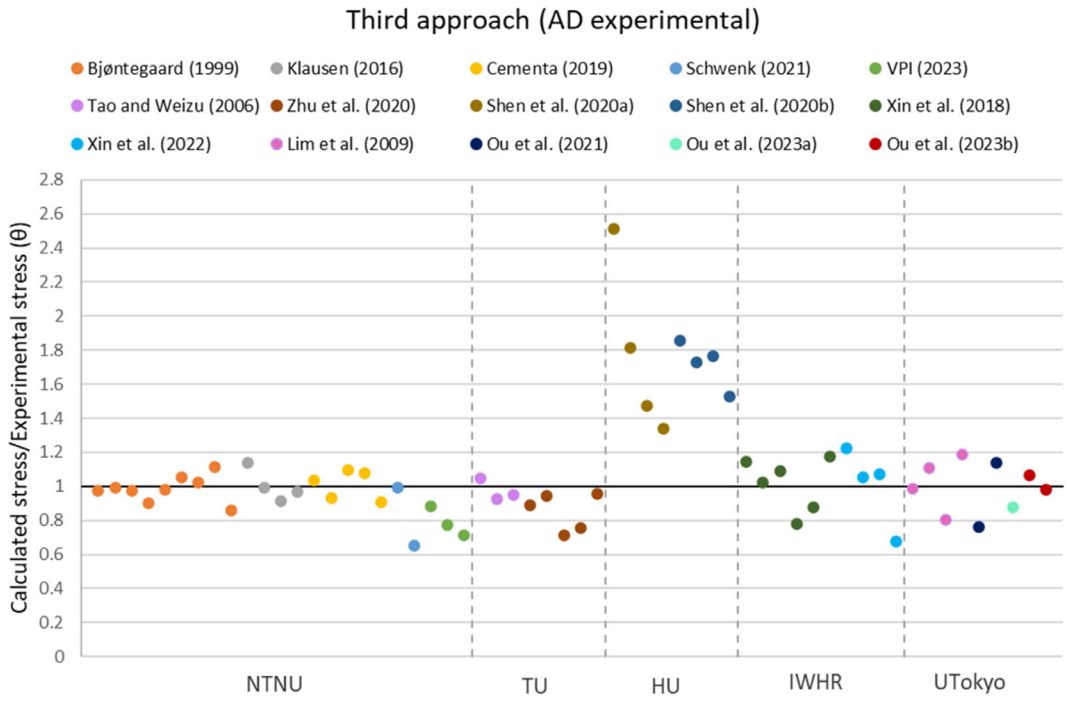

FIGURE 6 Calculated-to-experimental-stress ratio (θ) of the tests included in the reference database according to the third approach. The approach overestimates (underestimates) the experimental stress for $\theta > 1$ ($\theta < 1$). The tests are grouped in investigations (listed in the upper part of the figure), which are in turn arranged according to the institute they belong to. The reference institutes are separated by vertical dotted lines.

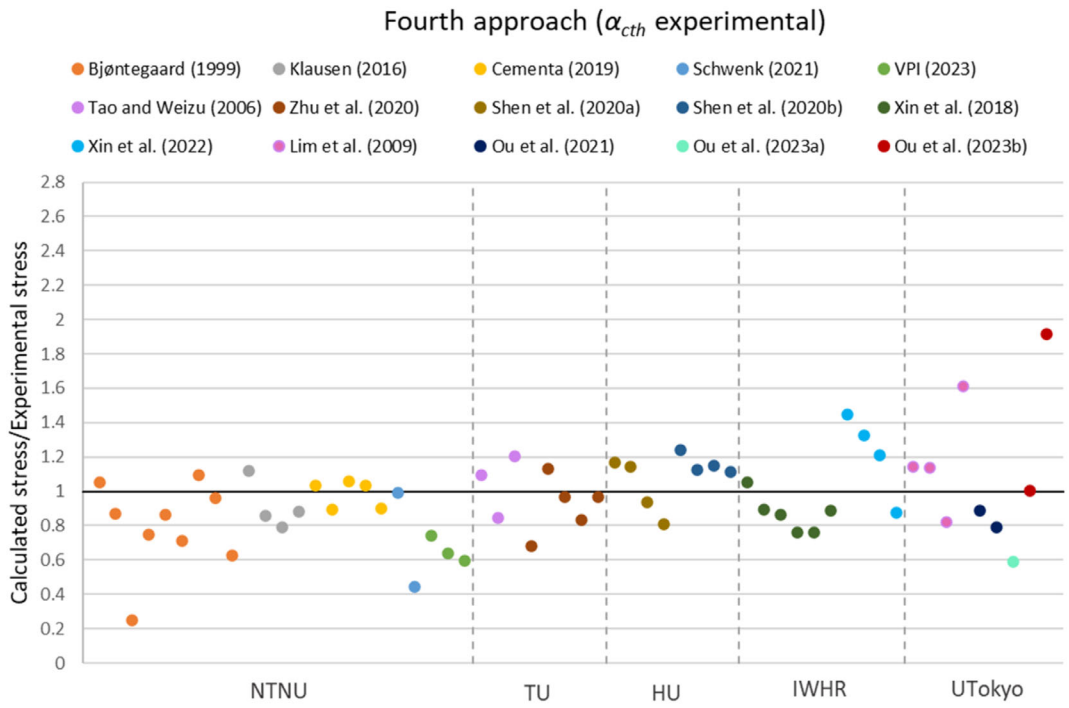

FIGURE 7 Calculated-to-experimental-stress ratio (θ) of the tests included in the reference database according to the fourth approach. The approach overestimates (underestimates) the experimental stress for $\theta > 1$ ($\theta < 1$). The tests are grouped in investigations (listed in the upper part of the figure), which are in turn arranged according to the institute they belong to. The reference institutes are separated by vertical dotted lines.

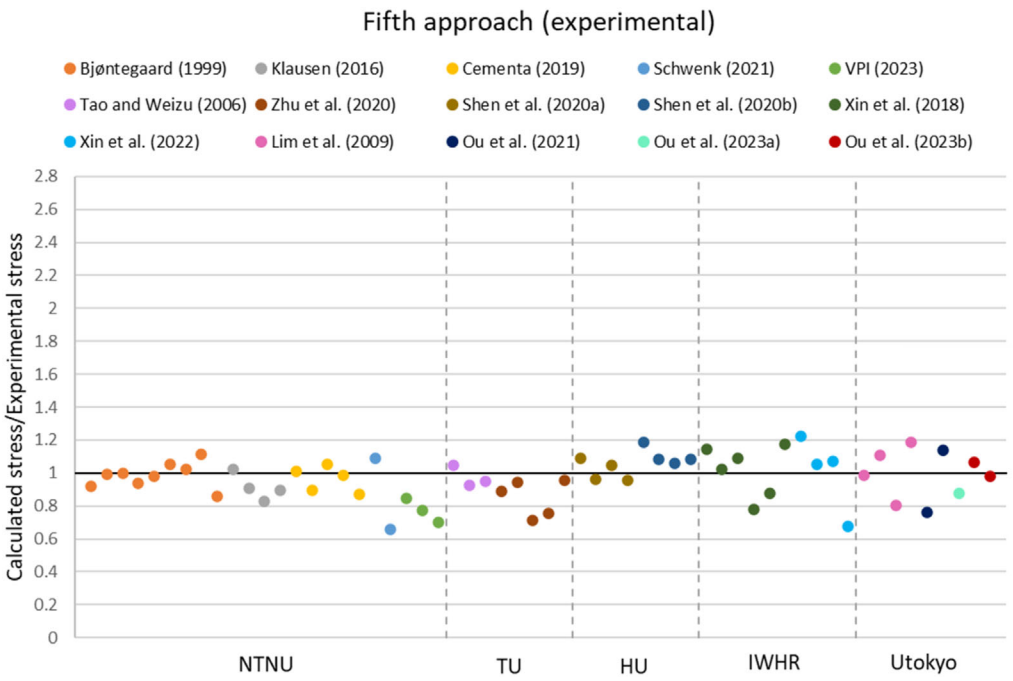

FIGURE 8 Calculated-to-experimental-stress ratio (θ) of the tests included in the reference database according to the fifth approach. The approach overestimates (underestimates) the experimental stress for $\theta > 1$ ($\theta < 1$). The tests are grouped in investigations (listed in the upper part of the figure), which are in turn arranged according to the institute they belong to. The reference institutes are separated by vertical dotted lines.

GGBFS ($\theta = 0.41$), respectively from Bjøntegaard[21] and Schwenk[27,28] investigations, stand out for being overly underestimated. This is most probably due to the high content of supplementary cementitious materials (SCMs) of the mixes (plus the low $w/b = 0.23$ of NTNU01_03_20%SF), that yield to experimental values of AD of two orders of magnitude greater than those given by Equation (7). The approach seems thus unable to predict this strong AD production.

The first approach results give good agreement with tests from TU, both in terms of average and distribution. However, $\sigma_1(t_{crit})$ measured for the HU tests is completely overestimated ($\mu_\theta = 1.78$ and $s_\theta = 0.40$). The high scatter is mostly due to the investigation by Shen et al. (2020),[34] conducted on tests with increasing GGBFS addition, while the high average value is due to both the HU investigations. Figure 4 shows that θ decreases with increasing SCMs presence but in this case, SM greatly overestimates the stress for all the tests, especially HU01_01_OPC ($\theta = 2.59$) and HU01_02_20%GGBFS ($\theta = 1.99$).

This trend recurs for the IWHR tests, with high $\mu_\theta = 1.30$ but acceptable s_θ. The tests are performed on FA concrete, with a constant 35% amount of FA in the investigation by Xin et al.,[36] and with increasing FA content in the one by Xin et al.[37] In this case, θ decreases with increasing FA presence, but θ is evidently influenced by other factors as well, since it varies also when FA is constant.

The high dispersion of the UTokyo results is probably caused by tests UTokyo01_04_7.5%EA ($\theta = 1.61$) and UTokyo04_02_10%EA ($\theta = 1.91$), including calcium sulfoaluminate as expansive agent.[41] In fact, when excluding these cases, s_θ is reduced from 0.40 to 0.19 for the UTokyo tests (Table 5).

The first approach can hence be considered satisfactorily accurate and in agreement with previous results by Reference 8, even though θ decreases with increasing SCMs content, and the approach is not able to predict the stress of mixes with high amounts of SCMs. Moreover, Bjøntegaard (1999) and Cementa (2019)—the only investigations where w/b was changed—showed the tendency for θ to decrease with decreasing w/b value. The data are however too limited to generalize this behavior.

3.3.2 | The second approach

In the second approach t_2 is assumed to be 2 days for all tests. Changing t_2 affects $E_c(t_2)$ and AD according to Equations (4) and (7), with E_c having greater weight in the stress evaluation (see section3.2). Moreover, the stress calculated by the second approach is expected to be

TABLE 5 Average value and standard deviation (μ_θ and s_θ, respectively) of θ calculated according to the five approaches for each investigation and institute.

		1st approach		2nd approach		3rd approach		4th approach		5th approach	
Institute	**Investigation**	μ_θ	s_θ	μ_θ	s_θ	μ_θ	s_θ	μ_θ	s_θ	μ_θ	s_θ
NTNU (Norway)	Bjøntegaard (1999)	0.80	0.26	0.84	0.30	0.99	0.07	0.80	0.24	0.99	0.07
	Klausen (2016)	1.00	0.14	0.99	0.14	1.00	0.08	0.91	0.12	0.91	0.07
	Cementa (2019)	1.07	0.08	1.04	0.08	1.01	0.08	0.99	0.07	0.96	0.07
	Schwenk (2022)	0.69	0.27	0.67	0.24	0.82	0.17	0.72	0.27	0.87	0.22
	VPI (2023)	0.69	0.09	0.68	0.08	0.79	0.07	0.66	0.06	0.77	0.06
	Total	**0.87**	**0.24**	**0.88**	**0.25**	**0.95**	**0.12**	**0.83**	**0.21**	**0.93**	**0.12**
TU (China)	Tao and Weizu (2006)	1.05	0.15	1.20	0.18	0.97	0.05	1.05	0.15	0.97	0.05
	Zhu et al. (2020)	0.92	0.15	0.70	0.12	0.85	0.10	0.92	0.15	0.85	0.10
	Total	**0.97**	**0.16**	**0.89**	**0.28**	**0.90**	**0.10**	**0.97**	**0.16**	**0.90**	**0.10**
HU (China)	Shen et al. (2020a)	1.79	0.55	1.66	0.62	1.79	0.45	1.01	0.15	1.01	0.06
	Shen et al. (2020b)	1.78	0.13	1.54	0.11	1.72	0.12	1.16	0.05	1.10	0.05
	Total	**1.78**	**0.40**	**1.60**	**0.45**	**1.75**	**0.33**	**1.09**	**0.13**	**1.06**	**0.07**
IWHR (China)	Xin et al. (2018)	1.13	0.13	0.90	0.09	1.01	0.14	0.87	0.10	1.01	0.14
	Xin et al. (2022)	1.57	0.21	1.11	0.16	1.01	0.20	1.21	0.21	1.01	0.20
	Total	**1.30**	**0.27**	**0.99**	**0.16**	**1.01**	**0.17**	**1.01**	**0.23**	**1.01**	**0.17**
UTokyo (Japan)	Lim et al. (2009)	1.18	0.28	1.18	0.28	1.02	0.14	1.18	0.28	1.02	0.14
	Ou et al. (2021)	0.84	0.05	0.76	0.10	0.95	0.19	0.84	0.05	0.95	0.19
	Ou et al. (2023a)	0.59	-	0.68	-	0.88	-	0.59	-	0.88	-
	Ou et al. (2023b)	1.46	0.45	1.69	0.40	1.02	0.04	1.46	0.45	1.02	0.04
	Total	**1.10**	**0.40**	**1.14**	**0.44**	**0.99**	**0.14**	**1.10**	**0.40**	**0.99**	**0.14**
Total		**1.12**	**0.43**	**1.04**	**0.40**	**1.07**	**0.33**	**0.96**	**0.26**	**0.97**	**0.13**

higher (lower) than that predicted by the first approach for t_{2exp} <2 days (t_{2exp} >2 days).

Figure 5 shows that changing t_2 does not impact significantly the stress calculated for the tests conducted at NTNU, HU, and UTokyo. However, it significantly increases the scatter for the TU tests (s_θ is 0.28 from 0.16). This is because μ_θ of the two TU investigations is respectively increased from 1.05 to 1.20 and decreased from 0.92 to 0.70 by the second approach, compared to the first one. The results are as expected since t_{2exp} <2 days (1 day in average) for the tests by Tao and Weizu,[32] and t_{2exp} >2 days (6.25 days in average) for the tests by Zhu et al.[33] Conversely, the approach predicted the tests performed at IWHR with much better average and s_θ than the first (μ_θ is now 0.99 from 1.30 and s_θ is 0.16 from 0.27).

The second approach provided expected results for all the tests included in the database, with significant difference from the first approach only when E_c varied more than 25% between the approaches, regardless of how much ΔAD changed. This showed that $t_2 = 2$ days can be assumed also for mixes with initial strong AD development, without modifying the accuracy of the method, as long as $1 < t_{2exp}$ <3.4 days (corresponding to the E_c limits). This recommended time range is not centered at 2 days due to the exponential nature of the E-modulus development function, whose rate influences the range width: more slowly E_c develops, the wider the range, and vice versa.

3.3.3 | The third approach

The first approach was not able to evaluate the stress of mixes with high amounts of SCMs, probably due to limits of the AD model (Equation 7) for mixes with cement types different than CEM I.[49] Moreover, many authors in the literature (e.g.,[20,21,45,50–52]) reported the inadequacy of current AD models for tests performed under varying temperature conditions, which is always the case at early ages. The third approach thus uses experimental values of AD as input to SM to evaluate the accuracy of Equation (7). It must be highlighted that EC2 recommends using equivalent age (maturity) in Equation (7) to

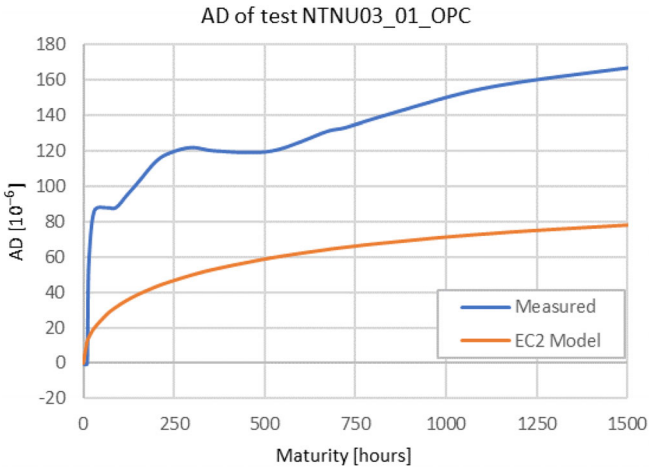

FIGURE 9 Measured and modeled (calculated by Equation 7) AD development of test NTNU03_01_OPC. Contraction is assumed positive.

consider the effects of varying temperature on AD. Maturity data were however provided only for some of the NTNU tests,[20,22–31] so to have homogeneous and comparable results, real time was used in Equation (7) for all the test results included in the reference database. Nonetheless, Figure 9 shows that Equation (7) is not able to predict the AD development even for test NTNU03_01_OPC (first test of the Cementa (2019) investigation) in which the equivalent time was used and the first approach returned accurate results.

Figure 6 and Table 5 show that the third approach has better accuracy than the first approach, especially in terms of s_0 (0.33 from 0.42). This holds true especially for mixes with high SCMs content—tests NTNU01_03_20% SF (θ is 0.97 from 0.22) by Bjøntegaard[21] and NTNU04_02_70%GGBFS (θ is 0.65 from 0.41) by Schwenk[27,28]—or with expansive agent—tests UTokyo01_04_7.5%EA (θ is 1.19 from 1.56) by Lim et al.[38] and UTokyo_04_02_10%EA (θ is 0.98 from 1.91) by Ou et al.[41]

However, $\sigma_1(t_{crit})$ still tends to decrease with increasing SCMs content, and the approach continues to not properly evaluate the stress for the HU tests.

An explanation to the first matter is that SCMs influence the whole concrete hydration chemistry, not only AD, and the current models (e.g., Equation 7) are based on Portland cement behavior. Hence, it could be expected that their accuracy decreases with increasing SCMs content in the mix.[2] Also, SCMs especially influence the heat evolvement of a concrete mix and hence its semi-adiabatic temperature history, under which the tests in the current database have been performed. This means that Equation (7) has even more difficulty in modeling the AD development of SCMs mixes under their semi-adiabatic temperature conditions, because of the coupling with the temperature variation.

Regarding the HU tests stress prediction, it should be remembered that AD produces EAC together with TD, which usually has a bigger role.[21] In this regard, the HU tests show very low experimental values of α_{cth} (Table 3), thus lower experimental values of TD than those calculated by SM. This affects the HU results much more than the inaccuracy of the AD model. This is also one of the reasons why $\sigma_1(t_{crit})$ of test NTNU03_01_OPC was accurately predicted by the first approach even though Equation (7) was not able to predict its AD development.

3.3.4 | The fourth approach

In the fourth approach, experimental values of α_{cth} (α_{exp}) are used as input to SM, instead of assuming $\alpha_{cth} = 10 \times 10^{-6}\,°C^{-1}$ (the $10^{-6}\,°C^{-1}$ part is omitted in the following for clarity reasons). α_{exp} was not provided in the literature for tests performed at TU and UTokyo. A value of 10 was hence assumed, making the fourth approach identical to the first for these tests.

The approaches are similar for the NTNU tests, with α_{exp} values close to 10. Conversely, very low values of α_{exp} (Table 3) were reported for the HU tests (in average 6.10), with values of 4.38 and 5.58 for tests HU01_01_OPC and HU01_02_20%GGBFS, respectively, whose stress is adequately predicted by the fourth approach but not by the first (θ is now 1.17 and 1.14, from 2.59 and 1.99). Also significant is the difference between the approaches for the IWHR tests ($\mu_\theta = 1.01$ from 1.30).

A reason for this behavior could be that the assumption $\alpha_{cth} = 10$ in SM was based on European experience[2] which differs in terms of materials and traditions from the Asian one.[53,54]

The fourth approach shows that it is better to use α_{exp} when available. If this is not possible, the assumption $\alpha_{cth} = 10$ in SM can be made considering that what actually influences $\sigma_1(t_{crit})$ is $TD = \alpha_{cth} \cdot \Delta T$, so the α_{cth} assumption shall consider the variation of ΔT.

In this regard, Figure 10 showed that the stress of the IWHR tests varied between the first and second approach even with moderate values of ΔT (between 6.50 and 15.70°C). Conversely, the NTNU test prediction did not change much regardless of the ΔT value. This means that for European mixes $\alpha_{cth} = 10$ can be safely assumed regardless of the ΔT value, but this results overly conservative for Asian mixes even in cases of low ΔT values. Based on the current database, $\alpha_{cth} = 7$ can be safely assumed for Asian mixes if α_{exp} is not available.

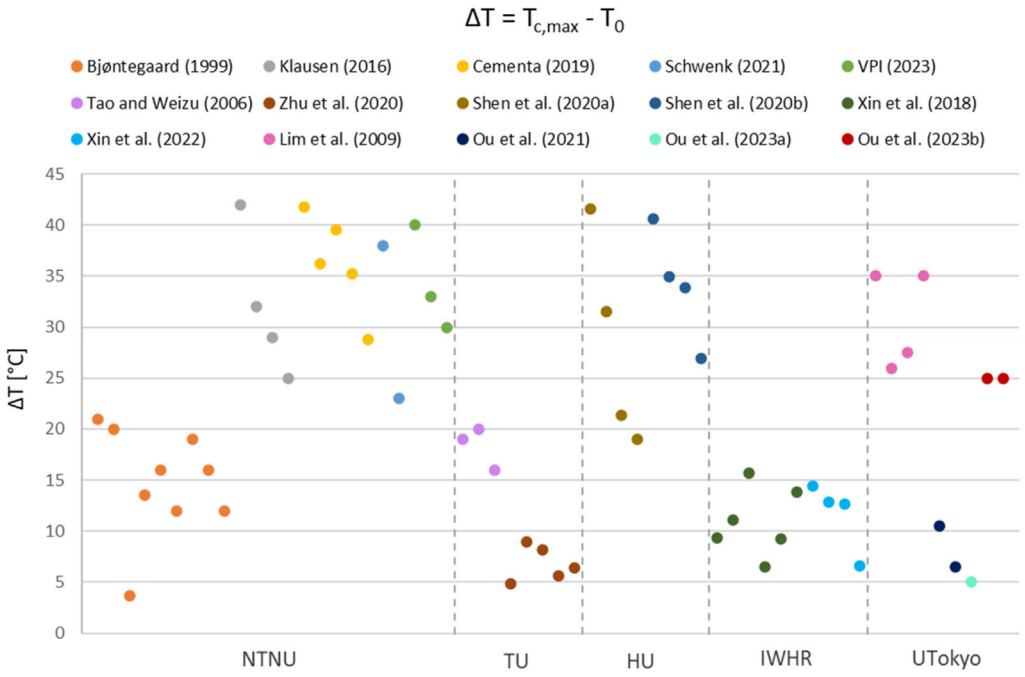

FIGURE 10 $\Delta T = T_{c,max} - T_0$ of the tests included in the reference database. The tests are grouped in investigations (listed in the upper part of the figure), which are in turn arranged according to the institute they belong to. The reference institutes are separated by vertical dotted lines.

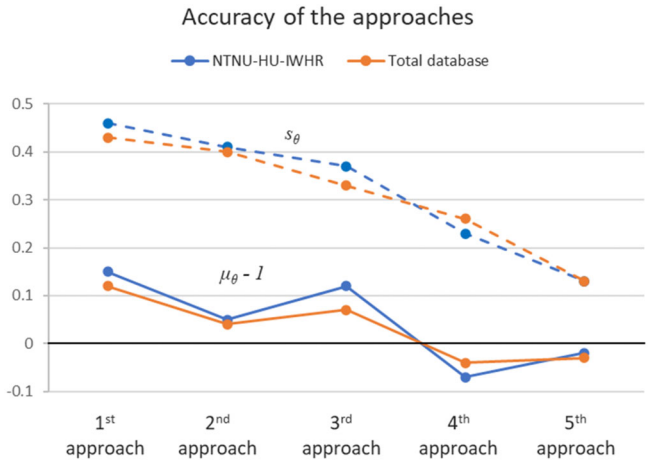

FIGURE 11 Accuracy of the five approaches in terms of $\mu_\theta - 1$ and s_θ. The accuracy increases if $\mu_\theta - 1$ and s_θ tend to zero. For $\mu_\theta - 1 > 0$ ($\mu_\theta - 1 < 0$) the approaches overestimate (underestimate) the stress development and hence the cracking risk. The values are shown for the total reference database and for the tests performed at NTNU, HU, and IWHR, for which $\propto_{exp} \neq 10^{-5}\,°C^{-1}$.

3.3.5 | The fifth approach

In the fifth approach, only experimentally determined inputs are used, leading to very good accuracy ($\mu_\theta = 0.97$ and $s_\theta = 0.13$) for the total database.

Figure 11 shows the variation in accuracy between the five approaches. Values of $\mu_\theta - 1$ and s_θ are presented for the total database and for the tests performed at NTNU, HU, and IWHR, for which $\alpha_{exp} \neq 10$. The optimum is reached for $\mu_\theta - 1$ and s_θ equal to zero. According to the figure, the accuracy increases with increasing approach number in terms of s_θ, but the second approach is the second with the best accuracy in terms of average.

This can be explained by associating the accuracy of each approach to how much their key parameter contributes to $\sigma_1(t_{crit})$. Assuming the first approach as reference, the second approach is related to t_2 (or better $E_c(t_2)$), the third to AD, the fourth to α_{cth} (or better TD), and the fifth to FD. Except for the second approach, the parameters are substituted with their experimental values in the other approaches. The accuracy of each approach related to the first, thus represents the accuracy of the parameter's model or assumption, and the influence of the parameter in the stress build-up.

Looking at Equation (4) and Figure 11, the highest accuracy (compared to the first approach) of the fifth approach means that FD is the parameter that contributes more to $\sigma_1(t_{crit})$, as expected, since FD is the driving force of the stress build-up process. FD is the sum of AD and TD, but AD alone influences $\sigma_1(t_{crit})$ less than TD, as showed by the accuracies of the third and fourth approaches. However, the sum of these two approaches accuracies (related to the first approach) is lower than the fifth approach accuracy, meaning that the way AD and TD combine to form FD needs further study to clarify the relation between the two parameters.

It is also worth mentioning that the fourth and fifth approach, despite their good accuracy, in average underestimate $\sigma_1(t_{crit})$ and thus R_{cr}. This is probably due to the stress assumptions in SM, which affect among others the creep development model. The underestimation is however not severe and is balanced by the 0.8 coefficient in Equation (1).

In the second approach, the assumption about t_2 leads to variations in $E_c(t_2)$ and AD. An assumed value of t_2, and consequently a somewhat assumed value of $E_c(t_2)$ and AD, are used in this approach. Hence, contrary to the results in Figure 11, we expect the second approach to show lower accuracy than the first, where $E_c(t_2)$ and AD are instead measured. Moreover, the second approach shows contradictory accuracies in terms of average and standard deviation. This makes the interpretation of the second approach more complex than the others, so three cases are considered:

a. The assumption about t_2 affects only AD, so $E_c(t_2) = E_c(t_{2exp})$. In this case, $\mu_\theta = 1.14$ and $s_\theta = 0.40$ for the whole database.
b. The assumption about t_2 affects only $E_c(t_2)$, so AD is calculated as in the first approach. In this case $\mu_\theta = 1.03$ and $s_\theta = 0.41$ for the whole database.
c. The assumption about t_2 affects both AD and $E_c(t_2)$. This is the current second approach, with $\mu_\theta = 1.04$ and $s_\theta = 0.40$ for the whole database.

Only case (a) shows expected accuracy values (lower than the first approach). Instead, cases (b) and (c) have very similar accuracy, proving that E_c is the key parameter of the second approach, but higher than the first approach. E_c(2 -days) was estimated by the authors for most of the tests, since insufficient data were provided in the literature to calculate E_c(2 days) with the EC2 model. The unexpected accuracy found for the second approach could therefore just be a coincidence produced by this estimation.

Nevertheless, Figure 11 and the discussion above highlighted that E_c contributes to the stress production more than AD and less than FD (approach with the best accuracy), but it is not clear whether E_c contributes more or less than TD. Still, according to the results presented in the current paper, SM looks able to capture and explain with reasonable simplicity and good accuracy the mechanisms and relations between the parameters involved in the early-age stress build-up.

4 | FIELD VERIFICATION

In this section, SM is applied to some well documented field cases on restrained concrete elements. The cases are briefly described, while the related input parameters for SM and the calculated R_{cr} are collected in Tables 6–8 and discussed at the end of the section.

4.1 | Field cases

4.1.1 | Case of the Civaux walls

During the construction of the Civaux nuclear power plant, two reinforced concrete walls were built to evaluate the risk of cracking of the containment at early ages.[55] The walls were 1.2 m wide, 1.9 m high, 20 m long, and were made with two different concrete mixes—an ordinary concrete (OC) and a high-performance concrete (HPC).[11]

TABLE 6 Input parameters used in SM for the Civaux walls and calculated cracking risk (R_{cr}).

Input parameter	OC	HPC	Notes
$R_{ax,1}$ (−)	0.5	0.5	Assumed according to Annex D
α_{cth} ($\times 10^{-6}$ °C^{-1})	10	10	Assumed according to Annex D
t_2 (days)	2	2	Assumed according to Annex D
t_{crit} (days)	5	5	Measured[55]
$E_c(t_2)$ (MPa)	30,000	34,000	Deduced from Reference 55
$T_{c,max} - T_0$ (°C)	59 − 15 = 44	46 − 15 = 31	Measured[55]
k_{Temp}	0.9	0.9	Assumed according to Annex D
$\varepsilon_{cbs}(t_{crit}) - \varepsilon_{cbs}(t_2)$ (−)	3.50E−05	1.50E−05	Provided in Reference 11
$\sigma_1(t_{crit})$ (MPa)	4.17	3.22	Calculated by SM
$f_{ct,eff}(t_{crit})$ (MPa)	2.5	3.2	Deduced from Reference 55
R_{cr} (−)	**2.09**	**1.26**	**Calculated by SM**

Note: The walls have same geometry, but are made with different concrete mixes—an ordinary concrete (OC) and a high performance concrete (HPC).
Abbreviation: SM, simplified method.

Input parameter	SV 40	Low heat	Notes
$R_{ax,1}$ (−)	0.5	0.5	Assumed according to Annex D
α_{cth} ($\times 10^{-6}$ °C^{-1})	10.4	8.4	Measured[56]
t_2 (days)	2.5	3	Measured[56]
t_{crit} (days)	6	7	Measured[56]
$E_c(t_2)$ (MPa)	29,100	31,300	Provided in Reference 56
$T_{c,max} - T_0$ (°C)	65–20 = 45	56–20 = 36	Measured[56]
k_{Temp}	0.78	0.8	Measured[56]
$\varepsilon_{cbs}(t_{crit}) - \varepsilon_{cbs}(t_2)$ (−)	2.0E–05	2.5E–05	Deduced in Reference 56
$\sigma_1(t_{crit})$ (MPa)	3.61	2.70	Calculated by SM
$f_{ct,eff}(t_{crit})$ (MPa)	3.70	2.91	Measured[56]
R_{cr} (−)	**1.22**	**1.16**	**Calculated by SM**

Note: The walls are made with different concrete mixes—a high performance concrete (SV 40) and a low heat concrete.
Abbreviation: SM, simplified method.

TABLE 7 Input parameters used in SM for the Bjørvika double-wall structure and calculated cracking risk (R_{cr}).

TABLE 8 Input parameters used in SM for beam RG8 studied in the CEOS project and calculated cracking risk (R_{cr}).

Input parameter	RG8	Notes
$R_{ax,1}$ (−)	0.55	Calculated[11]
α_{cth} ($\times 10^{-6}$ °C^{-1})	12	Measured[57]
t_2 (days)	2	Measured[57]
t_{crit} (days)	3	Measured[57]
$E_c(t_2)$ (MPa)	39,000	Provided in Reference 11
$T_{c,max} - T_0$ (°C)	53 − 21.5 = 31.5	Measured[57]
k_{Temp}	0.83	Provided in Reference 11
$\varepsilon_{cbs}(t_{crit}) - \varepsilon_{cbs}(t_2)$ (−)	1.0E − 05	Provided in Reference 11
$\sigma_1(t_{crit})$ (MPa)	4.5	Calculated by SM
$f_{ct,eff}(t_{crit})$ (MPa)	4.6	Provided in Reference 11
R_{cr} (−)	**1.22**	**Calculated by SM**

Abbreviation: SM, simplified method.

Thermocouples were embedded at various locations to follow the temperature evolution of the walls (Figure 12).

4.1.2 | Case of the Bjørvika walls

As part of the Bjørvika submerged tunnel project in Norway, a double-wall test structure (Figure 13) was built to evaluate the cracking risk at early ages of the low-heat concrete to be used in the tunnel.[56]

The structure consisted of two reinforced walls 2 m high, 1 m wide, and 15 m long, made of two different

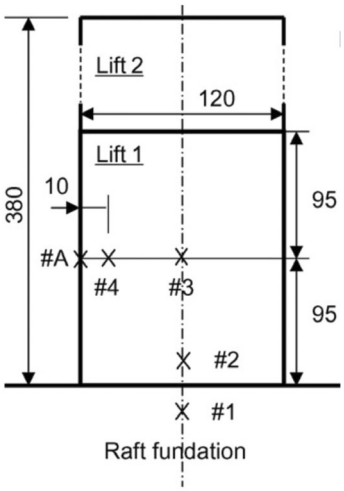

FIGURE 12 Geometry of the Civaux walls and locations of the embedded thermocouples. The dimensions are in cm.[55]

concrete mixes—a high performance concrete with 0.42 w/b (SV 40) and a low-heat concrete with 0.46 w/b, 36% FA and 5% SF (as percentage of binder weight). The walls were cast on a 2-week-old slab made with SV 40.

Vibrating wire strain gauges were embedded in two sections of the walls (Figures 13 and 14), to measure both temperature and strain. Mechanical properties and AD development were measured through parallel laboratory testing.[56]

4.1.3 | Case of the CEOS project beam

In the French national research project CEOS,[57] massive I-shaped beams composed of a central part (5.1 m long, 0.5 m wide, and 0.8 m high) and two massive heads

(0.9 m long, 2.2 m wide, and 0.9 m high) were tested (Figure 15) Two steel struts (diameter 32.4 cm and thickness 5.5 cm) were placed laterally between the heads to prevent almost all FD. The mentioned configuration allows to easily calculate $R_{ax,1}$ of the beam as the ratio between the stiffness of the struts and the stiffness of the struts plus that of the beam (Equation 2).

RG8[57] is the test considered herein, made with a Portland cement concrete mix (CEM I 52.5 N) with 0.46 w/b and 2% longitudinal reinforcement (Figure 16).

The specimen was fully instrumented, with thermocouples, vibrating wire extensometers on the struts and in the concrete, and electrical strain gauges on the reinforcement. From the strain measured on struts and reinforcement, it is possible, through elastic analysis, to exactly know the force in the struts and reinforcement, and to calculate that in the concrete by balancing the forces.

Mechanical properties and AD development were measured through parallel laboratory testing.[57]

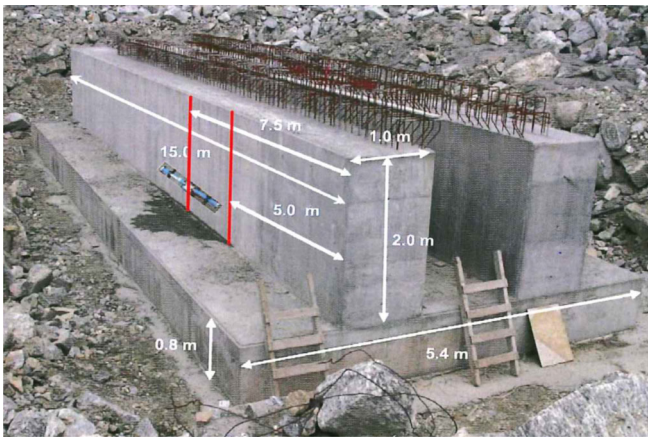

FIGURE 13 Geometry of the Bjørvika double-wall test structure.[56] The red lines represent the sections of the walls with embedded strain gauges.

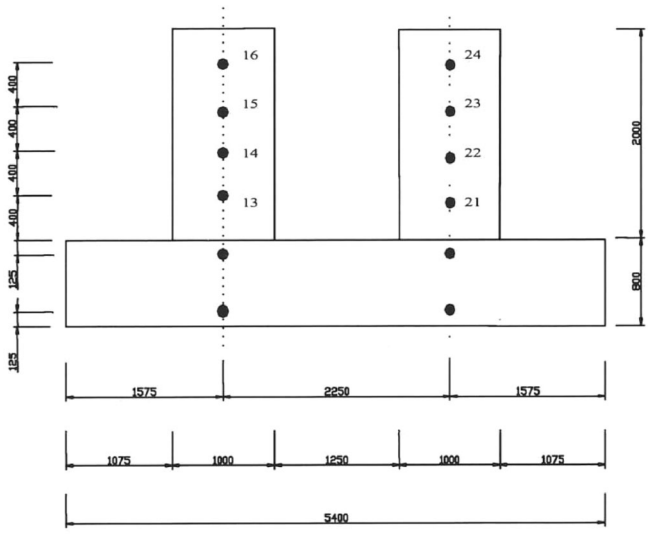

FIGURE 14 Middle cross-section of the double-wall structure and positioning of the strain gauges. Dimensions in mm.[56]

4.2 | Discussion

Table 6 presents the input values for SM and cracking risk of the Civaux walls. Both the used concretes show $R_{cr} > 1$, but with large difference between them, meaning that higher damage is expected with higher R_{cr}. This result is confirmed by the experimental crack pattern (Figure 17). The largest R_{cr} (OC) provided the highest number of cracks and the largest crack widths. This was expected since HPC was designed to have lower temperature increase (hence lower TD, see Table 6) than OC.

The same occurred for the Bjørvika test walls (Table 7), with the SV 40 concrete showing higher R_{cr} and higher damage than the low-heat one.[56]

Note that in the Bjørvika and CEOS cases (Table 8) the structures cracked even though $\sigma_1(t_{crit}) < f_{ct,eff}(t_{crit})$. This can be due to the assumptions of SM, but also to the numerous measuring difficulties in the field and the inhomogeneity of the concrete. In fact, in the CEOS case, the experimental stress was lower than $f_{ct,eff}(t_{crit})$. Buffo-Lacarrière et al.[57] attributed this matter to various causes: the scale effect of tensile strength,[58,59] the presence of dead weight and of a high number of sensors which produced a non-homogeneous stress profile in the central

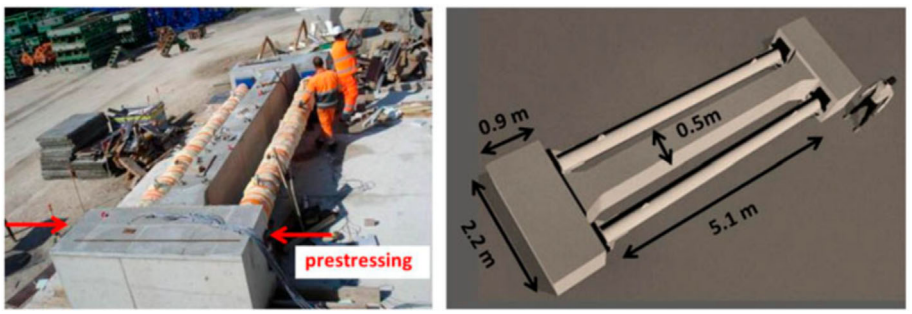

FIGURE 15 Geometry of the restrained beam specimens in the CEOS project.[57]

section of the restrained beam, the temperature gradient in the section during hydration, and creep-induced micro damage.

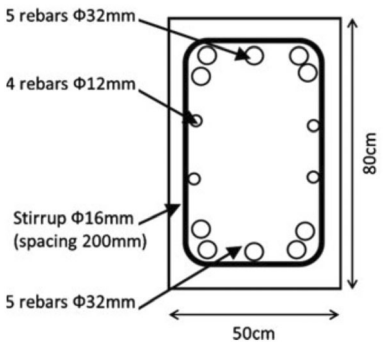

FIGURE 16 Reinforcement of beam RG8. The cover is 30 mm (50 mm for longitudinal rebars).[57]

Moreover, Figure 18 shows that the average experimental-failure-stress-to-experimental-tensile-strength ratio of the cracked TSTM specimens included in the current database is 0.81, instead of being greater than 1. This means that the measured failure stress is in average approx. 20% lower than the tensile strength, and that this deviation cannot be attributed to the inaccuracies of SM.

This is most probably due to different test conditions in the test methods used to measure $f_{ct,eff}(t_{crit})$ and $\sigma_1(t_{crit})$.[8,33,36] The tensile strength can be measured by direct tension or splitting tests (converted into direct tensile strength values in this paper). In both cases, virgin, relatively small specimens are rapidly loaded until failure. On the other hand, $\sigma_1(t_{crit})$ is measured in the TSTM, where the specimen (measuring length up to 1500 mm, see Table 1) is subjected to sustained loading from an

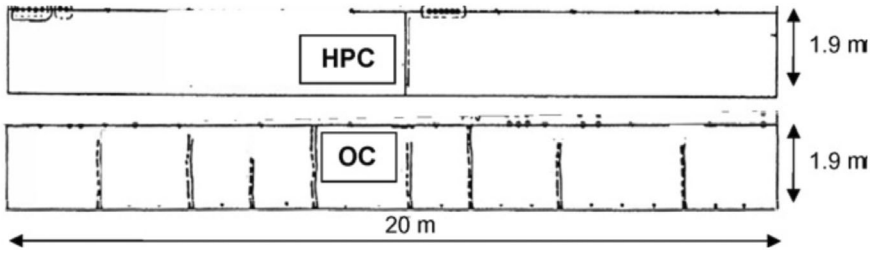

FIGURE 17 Crack pattern of OC (at the bottom) and HPC (at the top) walls on site (Ithurralde, 1989). The cracks are represented by a straight line. Eight major cracks have been noticed for the OC (1 × 40 μm + 4 × 100 μm + 2 × 200 μm + 1 × 500 μm). One major cracks has been noticed for the HPC (1 × 100 μm).[55] HPC, high-performance concrete; OC, ordinary concrete.

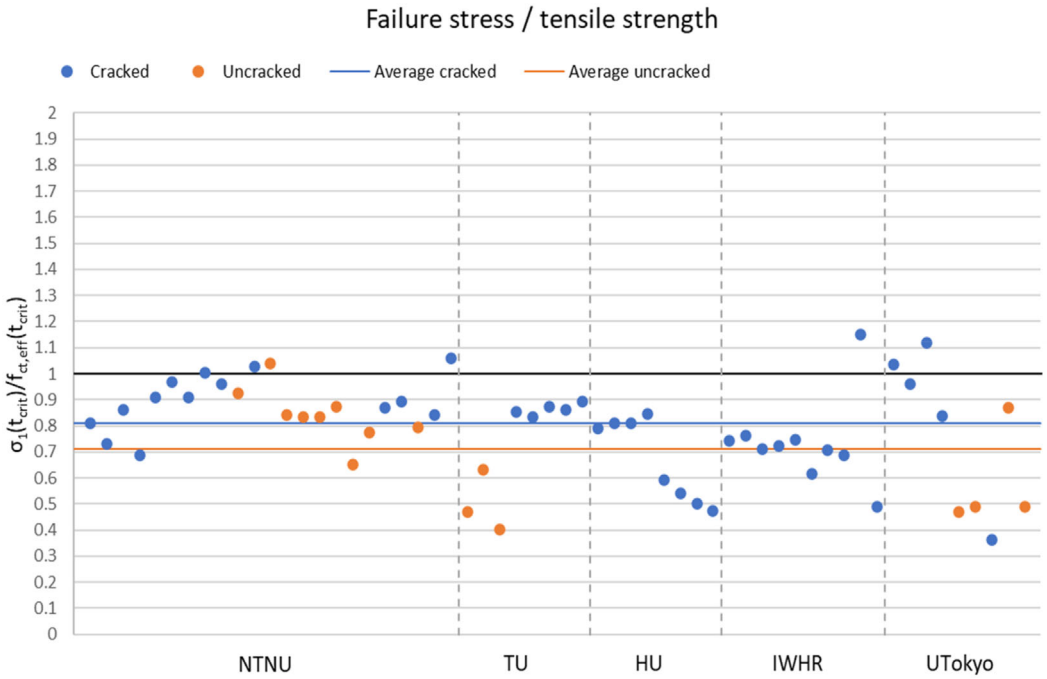

FIGURE 18 Experimental failure stress/tensile strength ratio of the tests included in the reference database. The tests are divided in two series according to whether they cracked or not, and are grouped in reference institutes separated by vertical dotted lines.

early age until final testing. Under sustained loading, tertiary creep damage[60] can occur, decreasing the failure-stress-to-tensile-strength ratio both in compression[61–65] and in tension.[66,67] Furthermore, microcracking is generated due to temperature variations and displacement adjustments to keep R_{cr} constant, resulting in fatigue and internal damage accumulation,[36] hence decreasing $\sigma_1(t_{crit})$.

Another parameter contributing to the premature failure of the TSTM tests is a possible eccentricity of the load applied by the TSTM,[8] which is more significant than that occurring during the measurement of $f_{ct,eff}(t_{crit})$ due to the different specimen dimensions. The eccentricity effect on $\sigma_1(t_{crit})$ has been investigated by Reference 33 at TU, where the multi-TSTM system allowed to parallelly measure both stress and strength in two identical TSTM rigs, so that the asymmetry effects on $\sigma_1(t_{crit})$ and $f_{ct,eff}(t_{crit})$ were identical. The study concluded that the eccentricity was not the primary cause of lower failure stress.

The lower cracking stress is hence a product of sustained loading, tertiary creep, and temperature variations occurring during the stress-build-up process and must be accounted for in the evaluation of R_{cr}. In the case of Annex D,[2] this is considered by the coefficient 0.8 in Equation (1). Alternatively, CIRIA CT66[3] recommends to replace $f_{ct,eff}(t_{crit})$ with the characteristic tensile strength, equal to 0.7 times the average tensile strength recommended by Reference 2.

5 | CONCLUSIONS

The Annex D of the new EC2 includes a simplified method (SM) to estimate the stresses generated when the deformations of concrete are restrained by boundary conditions. In this paper, SM was verified against laboratory tests performed in various TSTMs, and three field cases of restrained real structures at early ages.

In the laboratory verification, SM was applied according to five approaches considering different available inputs (assumed, measured, or modeled). In the field verification, SM was used to calculate the cracking risk (R_{cr}) of the structures with the available inputs.

The stress ($\sigma_1(t_{crit})$) calculated by SM for the TSTM tests was compared to the experimental stress for each approach, and R_{cr} of the structures was related to the observed crack pattern, leading to the following considerations pertaining the current database:

- The accuracy of SM varies depending on the type of available inputs and on the accuracy of the models used to describe them. However, it is in general very good, especially when experimentally determined inputs are used.
- The fourth and fifth approaches slightly underestimated $\sigma_1(t_{crit})$ and hence R_{cr}, despite their good accuracy. This is probably due to the SM stress assumptions, that are however balanced by the 0.8 coefficient in Equation (1). SM can thus be safely adopted.
- The method tended to give lower $\sigma_1(t_{crit})$ with increasing SCMs content. This is because SCMs influence the whole chemistry of hardening concrete, moving away from the behavior predicted by current Portland-based models. It is hence easily expected that their accuracy decreases the more SCMs the mix contains. It is therefore recommended to update the models implemented in SM, so that they can describe SCMs-based mixes especially under varying temperature conditions which are always the case at early ages.
- The SM can capture and explain with reasonable simplicity the mechanisms and relations between the parameters involved in the stress build-up during early ages. The accuracy of each approach gives in fact an indication of how much the parameters contribute to the stress. The most important is the FD, the driving force of the phenomenon. FD is the sum of TD and AD, with TD contributing more than AD to the stress. It is thus of interest to further investigate how AD and TD combine to form FD. The stiffness of the concrete element, represented by the E-modulus, contributes to $\sigma_1(t_{crit})$ more than AD and less than FD, but it was not possible to determine its relationship with TD due to lack of data in the current database.
- The calculated R_{cr} well indicated the extent of the damage in the field cases, with higher R_{cr} corresponding to more severe damage.
- Three out of five studied structures cracked even for stress values lower than the tensile strength, and the failure stress of the failed TSTM tests was in average 20% lower than the tensile strength. The difference does not seem to be related to SM but it was attributed to measuring difficulties on site, inhomogeneous nature of concrete, and different test conditions in the test methods used to measure the stress and the strength in the laboratory (size effect, sustained loading, tertiary creep, temperature variations).

DATA AVAILABILITY STATEMENT

The data that support the findings of this study are available from the corresponding author upon reasonable request.

ORCID

Antonia Menga https://orcid.org/0000-0001-7349-1726
Jean-Michel Torrenti https://orcid.org/0000-0003-0467-4371

Anja Birgitta Estensen Klausen https://orcid.org/0000-0002-0888-5769

REFERENCES

1. Kanstad T, Klausen ABE, Menga A. Background document to FprEN 1992-1-1 2023 annex D: evaluation of early-age and long-term cracking due to restraint. CEN/-TC250/SC2/WG1/TG7. 2023.
2. CEN/TC 250. EN 1992-1-1: Eurocode 2: Design of concrete structures – Part 1-1: General rules and rules for buildings, bridges and civil engineering structures, Annex D. November; 2023. p 271–5.
3. Kanavaris F, Kaethner S. CIRIA guide C766: an overview of the updated CIRIA C660 guidance on control of cracking in reinforced concrete structures. In International RILEM Conference on Sustainable Materials, Systems and Structures—SMSS192019. March; 2019.
4. Azenha M, Kanavaris F, Schlicke D, Jędrzejewska A, Benboudjema F, Honorio T, et al. Recommendations of RILEM TC 287-CCS: thermo-chemo-mechanical modelling of massive concrete structures towards cracking risk assessment. Mater Struct. 2021;54(4):135. https://doi.org/10.1617/s11527-021-01732-8
5. Jędrzejewska A, Zych M, Kanavaris F, Chen F, Ito S, Torrenti JM, et al. Standardized models for cracking due to restraint of imposed strains—the state of the art. Struct Concr. 2023;24:5388–405. https://doi.org/10.1002/suco.202200301
6. Torrenti J-M. Basic creep of concrete-coupling between high stresses and elevated temperatures. Eur J Environ Civ Eng. 2018;22(12):1419–28. https://doi.org/10.1080/19648189.2017.1280417
7. Larson M. Estimation of crack risk in early age concrete: simplified methods for practical use. Doctoral Dissertation. Luleå Tekniska Universitet. 2000.
8. Bjøntegaard Ø. Basis for and practical approaches to stress calculations and crack risk estimation in hardening concrete structures – state of the art. FA 3 technical performance. SP 3.1 crack free concrete structures. Norway: SINTEF Building and Infrastructure; 2011.
9. Kanstad T. Verification of three different calculation methods for early age concrete. Crack risk assessment of hardening concrete structures. Sweden: The Nordic Concrete Federation; 2006. p. 101–10. ISBN:82-91341-97-4.
10. Menga A, Kanstad T, Klausen ABE. Evaluation of early age cracking due to restraint: verification of the simplified stress calculation method proposed in prEN 1992-1-1. Proceedings of the 6th Fib International Congress in Oslo, Norway; 2022.
11. Torrenti J-M. Analysis of the annex D of the future EC2 "evaluation of early-age and long-term cracking due to restraint". Proceedings of the 6th fib international congress in Oslo, Norway; 2022.
12. Trost H. Implications of the superposition principle in creep and relaxation problems for concrete and prestressed concrete. Beton Stahlbetonbau. 1967;62(10):230–8.
13. Jędrzejewska A, Zych M, Torrenti JM, Kanavaris F, Azenha M, Chen F, et al. Practical insights on standardised models for estimation of crack width due to imposed strains in edge-restrained reinforced concrete elements. Eng Struct. 2024;305:117757. https://doi.org/10.1016/j.engstruct.2024.117757
14. Bentur A, Kovler K. Evaluation of early age cracking characteristics in cementitious systems. Mater Struct. 2003;36:183–90. https://doi.org/10.1007/BF02479556
15. Kanavaris F, Azenha M, Schlicke D, Kovler K. Longitudinal restraining devices for the evaluation of structural behaviour of cement-based materials: the past, present and prospective trends. Strain. 2020;56(3):e12343. https://doi.org/10.1111/str.12343
16. Delsaute B, Staquet S. Testing concrete since setting time under free and restrained conditions. Advanced techniques for testing of cement-based materials; Cham: Springer Nature Switzerland; 2020. p. 177–209. https://doi.org/10.1007/978-3-030-39738-8_6
17. Baron J. Properties of set concrete at early ages state-of-the-art-report. Mater Struct. 1981;14:399–450. https://doi.org/10.1007/BF02476348
18. Kamen A, Denarié E, Sadouki H, Brühwiler E. Thermo-mechanical response of UHPFRC at early age – experimental study and numerical simulation. Cem Concr Res. 2008;38(6):822–31. https://doi.org/10.1016/j.cemconres.2008.01.009
19. Shi N, Ouyang J, Zhang R, Huang D. Experimental study on early-age crack of mass concrete under the controlled temperature history. Adv Mater Sci Eng. 2014;2014:1–10. https://doi.org/10.1155/2014/671795
20. Klausen ABE. Early age crack assessment of concrete structures. Experimental investigation of decisive parameters. Doctoral thesis. Norway: Norwegian University of Science and Technology (NTNU); 2016.
21. Bjøntegaard Ø. Thermal dilation and autogenous deformation as driving forces to self-induced stresses in high performance concrete. Doctoral thesis. Norway: Norwegian University of Science and Technology (NTNU); 1999.
22. Skjølsvold O. Determination of parameters for CrackTestCoin – Norcem Anleggsement SR – w/c = 0.38, Test report, Norway: SINTEF Building and Infrastrcture; 2019.
23. Skjølsvold O. Determination of parameters for CrackTestCoin – Cementa Anlägningscement FA – v/c = 0.38, Test report, Norway: SINTEF Building and Infrastrcture; 2019.
24. Skjølsvold O. Determination of parameters for CrackTestCoin – Cementa Anlägningscement – v/c = 0.38, Test report, Norway: SINTEF Building and Infrastrcture; 2019.
25. Skjølsvold O. Determination of parameters for CrackTestCoin – Norcem Anleggsement SR – v/c = 0.48, Test report, Norway: SINTEF Building and Infrastrcture; 2019.
26. Skjølsvold O. Determination of parameters for CrackTestCoin – Cementa Anlägningscement FA – v/c = 0.48, Test report, Norway: SINTEF Building and Infrastrcture; 2019.
27. Menga A. Determination of parameters for CrackTest COIN-Schwenk CEM III/B 42.5 L-LH/SR (na) – w/c = 0.45, Test report, Norway: NTNU; 2022.
28. Menga A. Determination of parameters for CrackTest COIN-Schwenk Miljøsement CEM II/B-S 52.5 N – w/c = 0.45, Test report, Norway: NTNU; 2022.
29. Menga A. Determination of parameters for CrackTest COIN-Norcem Anlegg CEM I 52.5 N – w/c = 0.40, Test report, Norway (to be published).
30. Menga A. Determination of parameters for CrackTest COIN-Norcem Anlegg CEM I 52.5 N + 17% VPI – w/b = 0.40, Test report, Norway (to be published).
31. Menga A. Determination of parameters for CrackTest COIN-Norcem Anlegg CEM I 52.5 N + 33% VPI – w/b = 0.40, Test report, Norway (to be published).

32. Tao Z, Weizu Q. Tensile creep due to restraining stresses in high-strength concrete at early ages. Cem Concr Res. 2006; 36(3):584–91. https://doi.org/10.1016/j.cemconres.2005.11.017
33. Zhu H, Hu Y, Li Q, Ma R. Restrained cracking failure behaviour of concrete due to temperature and shrinkage. Constr Build Mater. 2020;244:118318. https://doi.org/10.1016/j.conbuildmat.2020.118318
34. Shen D, Jiao Y, Gao Y, Zhu S, Jiang G. Influence of ground granulated blast furnace slag on cracking potential of high performance concrete at early age. Constr Build Mater. 2020;241:117839. https://doi.org/10.1016/j.conbuildmat.2019.117839
35. Shen D, Kang J, Jiao Y, Li M, Li C. Effects of different silica fume dosages on early-age behaviour and cracking resistance of high strength concrete under restrained condition. Constr Build Mater. 2020;263:120218. https://doi.org/10.1016/j.conbuildmat.2020.120218
36. Xin J, Zhang G, Liu Y, Wang Z, Wu Z. Effect of temperature history and restraint degree on cracking behavior of early-age concrete. Constr Build Mater. 2018;192:381–90. https://doi.org/10.1016/j.conbuildmat.2018.10.066
37. Xin J, Liu Y, Zhang G, Wang Z, Wang J, Yang N, et al. Evaluation of early-age thermal cracking resistance of high w/b, high volume fly ash (HVFA) concrete using temperature stress testing machine. Case Stud Constr Mater. 2022;16:e00825. https://doi.org/10.1016/j.cscm.2021.e00825
38. Lim S, Lin Z, Kishi T. Early-age creep of fly ash, blast furnace slag, and expansive concretes. Creep, shrinkage and durability mechanics of concrete and concrete structures, two volume set: Proceedings of the CONCREEP 8 conference; 2008 September 30–October 2; Ise-Shima, Japan. CRC Press; 2008. https://doi.org/10.1201/9780203882955.ch42
39. Ou G, Kishi T, Lin Z, Kamada T. Theoretical modeling and evaluation of thermal stress evolution of concrete at early age by temperature stress testing machine. EASEC16: Proceedings of the 16th East Asian-Pacific Conference on Structural Engineering and Construction, 2019. Singapore: Springer; 2021. https://doi.org/10.1007/978-981-15-8079-6_163
40. Ou G, Lin Z, Kishi T. The practical application of a self-developed temperature stress testing machine in development of expansive concrete blended with calcium sulfoaluminate additives. Cem Concr Res. 2023;164:107045. https://doi.org/10.1016/j.cemconres.2022.107045
41. Ou G, Kishi T, Mo L, Lin Z. New insights into restrained stress and deformation mechanisms of concretes blended with calcium sulfoaluminate and MgO expansive additives using multi-scale techniques. Constr Build Mater. 2023;371:130737. https://doi.org/10.1016/j.conbuildmat.2023.130737
42. Klausen AEB, Kanstad T, Bjøntegaard Ø. Updated temperature-stress testing machine (TSTM): introductory tests, calculations, verification, and investigation of variable fly ash content. CONCREEP 10; 2015. p. 724–32. https://doi.org/10.1061/9780784479346.086
43. Zhu H, Li Q, Hu Y. Self-developed testing system for determining the temperature behaviour of concrete. Materials. 2017; 10(4):419. https://doi.org/10.3390/ma10040419
44. Shen D, Jiang J, Shen J, Yao P, Jiang G. Influence of curing temperature on autogenous shrinkage and cracking resistance of high-performance concrete at an early age. Constr Build Mater. 2016;103:67–76. https://doi.org/10.1016/j.conbuildmat.2015.11.039
45. EN 1992-1-1:2004. Eurocode 2: design of concrete structures – part 1-1: general rules and rules for buildings. London: British Standard Institution; 2005. p. 659–68.
46. Kanstad T, Hammer TA, Bjøntegaard Ø, Sellevold EJ. Mechanical properties of young concrete: Part I: experimental results related to test methods and temperature effects. Mater Struct. 2003;36:218–25. https://doi.org/10.1007/bf02479614
47. Chromiński K, Tkacz M. Comparison of outlier detection methods in biomedical data. J Med Inform Technol. 2010;16: 89–94.
48. Bjøntegaard Ø, Martius-Hammer TA, Krauss M, Budelmann H. Round Robin documentation report: program, test results and statistical evaluation. RILEM Technical Committee 195-DTD recommendation for test methods for AD and TD of early age concrete. Dordrecht: Springer; 2014. p. 1–47. https://doi.org/10.1007/978-94-017-9266-0_1
49. fib special activity group NMC, Taerwe L, Matthys S. fib model code for concrete structures 2010. Vol XXXI. Berlin, Germany: Ernst & Sohn, Wiley; 2013. p. 402. https://doi.org/10.1002/9783433604090
50. Tazawa E, Miyazawa S. Influence of cement and admixture on autogenous shrinkage of cement paste. Cem Concr Res. 1995; 25(2):281–7. https://doi.org/10.1016/0008-8846(95)00010-0
51. Jonasson J, Hedlund H. An engineering model for creep and shrinkage in high performance concrete. Reunion Internationale des Laboratoires D'essais et de Recherches sur les Materiaux et les constructions (RILEM) proceedings, shrinkage of concrete; Champs sur Marne: RILEM Publications SARL; 2000. p. 507–29.
52. Lee K, Lee H, Lee S, Kim G. Autogenous shrinkage of concrete containing granulated blast-furnace slag. Cem Concr Res. 2006; 36(7):1279–85. https://doi.org/10.1016/j.cemconres.2006.01.005
53. Lai W. L., Kou S. Why does Africa need African concrete? An observation of concrete in Europe, America, and Asia–and conclusions for Africa. Johannesburg: International Conference on Advances in Cement and Concrete Technology in AfricaAt; 2013.
54. CS (Chinese Standard) GB 175-2007/XG1-2009. Common Portland cement, quality, quality supervision inspection and quarantine of the People's Republic of China. China: Standardization Administration of the People's Republic China; 2009 (in Chinese).
55. Benboudjema F, Torrenti J-M. Early-age behaviour of concrete nuclear containments. Nucl Eng Des. 2008;238(10):2495–506. https://doi.org/10.1016/j.nucengdes.2008.04.009
56. Ji G. Cracking risk of concrete structures in the hardening phase: experiments, material modeling and finite element analysis. Doctoral thesis. Norway: Norwegian University of Science and Technology (NTNU); 2008.
57. Buffo-Lacarrière L, Baron S, Barré F, Chauvel D, Darquennes A, Dubois JP, et al. Restrained shrinkage of massive reinforced concrete structures: results of the project CEOS. fr. Eur J Environ Civ Eng. 2015;20:785–808. https://doi.org/10.1080/19648189.2015.1072587
58. Rossi P, Wu X, Le Maou F, Belloc A. Scale effect on concrete in tension. Mater Struct. 1994;27:437–44. https://doi.org/10.1007/bf02473447
59. Sellier A, Millard A. Weakest link and localisation WL2: a method to conciliate probabilistic and energetic scale effects in numerical models. Eur J Environ Civ Eng. 2014;18(10):1177–91. https://doi.org/10.1080/19648189.2014.906368

60. Brachmann G, Oettel V, Empelmann M. Background investigation and comparative calculations relating to Eurocode 2 as part of the evaluation of the national annexes – Background investigation of the coefficients α_{cc} and α_{ct}. CEN/TC 250/SC 2/WG 1 N 440. 2016 June 30.
61. Rüsch H. Researches toward a general flexural theory for structural concrete. J Am Concr Inst. 1960;57(1):1–28. https://doi.org/10.14359/8009
62. Rüsch H. Versuche zur Bestimmung des Einflusses der Zeit auf Festigkeit und Verformung. Munchen: IABSE Kongressbericht, Technische Hochschule München; 1956 (in German).
63. Grasser E. Darstellung und kritische Analyse der Grundlagen für eine wirklichkeitsnahe Bemessung von Stahlbetonquerschnitten bei einachsigen Spannungszuständen. Dissertation. Munchen: Fakultät für Bauwesen, TH München; 1968 (in German).
64. Rüsch H, Grasser E, Rao PS. Grundlagen für die Bemessung bei einachsigen Spannungszuständen im Betonbau. MPA für das Bauwesen der TH München, Bericht Nr. 47. 1961 (in German).
65. Wittmann F, Zaitsev J. Verformung und Bruchvorgang poröser Baustoffe bei kurzzeitiger Belastung und Dauerlast. Deutscher Ausschuss für Stahlbeton, Heft 232. Berlin: Ernst & Sohn; 1974 (in German).
66. Al-Kubaisy MA, Young AG. Failure of concrete under sustained tension. Mag Concr Res. 1975;27(92):171–8. https://doi.org/10.1680/macr.1975.27.92.171
67. Reinhardt H. W., Cornelissen H. A. W. Zeitstandzugversuche in Beton. Baustoffe ´85; Bauverlag, Wiesbaden, Gütersloh: Bauverlag GmbH· Wiesbaden und Berlin; 1985 (in German).

AUTHOR BIOGRAPHIES

Antonia Menga, Ph.D. Student, Department of Structural Engineering, Norwegian University of Science and Technology (NTNU), Trondheim, Norway. Email: antonia.menga@ntnu.no

Jean-Michel Torrenti, Professor, Université Gustave Eiffel, Paris, France; Dean of Research, ESITC-Paris, Arcueil, France. Email: jean-michel.torrenti@univ-eiffel.fr

Terje Kanstad, Professor, Department of Structural Engineering, Norwegian University of Science and Technology (NTNU), Trondheim, Norway. Email: terje.kanstad@ntnu.no

Anja Birgitta Estensen Klausen, Associate Professor, Department of Structural Engineering, Norwegian University of Science and Technology (NTNU), Trondheim, Norway. Email: anja.klausen@ntnu.no

How to cite this article: Menga A, Torrenti J-M, Kanstad T, Klausen ABE. Early-age cracking due to restraint: Laboratory and field investigations on the predictive capacity of the simplified method in Annex D of the future EC2. Structural Concrete. 2024. https://doi.org/10.1002/suco.202400173